Chem Soc Rev

TUTORIAL REVIEW

View Article Online
View Journal | View Issue

Cite this: *Chem. Soc. Rev.*, 2023, **52**, 5827

Current trends in the detection and removal of heavy metal ions using functional materials

Meng Li, *[a] Quanyu Shi,[a] Ningxin Song,[a] Yumeng Xiao,[a] Lidong Wang,[a] Zhijun Chen *[b] and Tony D. James *[cd]

The shortage of freshwater resources caused by heavy metal pollution is an acute global issue, which has a great impact on environmental protection and human health. Therefore, the exploitation of new strategies for designing and synthesizing green, efficient, and economical materials for the detection and removal of heavy metal ions is crucial. Among the various methods for the detection and removal of heavy ions, advanced functional systems including nanomaterials, polymers, porous materials, and biomaterials have attracted considerable attention over the past several years due to their capabilities of real-time detection, excellent removal efficiency, anti-interference, quick response, high selectivity, and low limit of detection. In this tutorial review, we review the general design principles underlying the aforementioned functional materials, and in particular highlight the fundamental mechanisms and specific examples of detecting and removing heavy metal ions. Additionally, the methods which enhance water purification quality using these functional materials have been reviewed, also current challenges and opportunities in this exciting field have been highlighted, including the fabrication, subsequent treatment, and potential future applications of such functional materials. We envision that this tutorial review will provide invaluable guidance for the design of functional materials tailored towards the detection and removal of heavy metals, thereby expediting the development of high-performance materials and fostering the development of more efficient approaches to water pollution remediation.

Received 6th May 2023

DOI: 10.1039/d2cs00683a

rsc.li/chem-soc-rev

Key learning points

A. Introduction to the hazards of heavy metal ion pollution and the necessity of water treatment.
B. Advantages and disadvantages of different materials for the detection and removal of heavy metal ions.
C. Applications of functional materials for wastewater treatment.
D. Current challenges and future developments.

1. Introduction

With the advancement of industrialization, global demand for fresh water globally is expected to increase by 55% between 2000 and 2050. However, the contamination of water by heavy metal ions further exacerbates the current situation.[1–3] For instance, mercury ions, a commonly occurring bioaccumulative heavy metal ion pollutant, pose a significant threat to human health and environmental ecology. Mercury is predominantly generated by various anthropogenic activities such as coal combustion, battery production, and waste incineration. Most of the harmful Hg^{2+} ions are distributed in aqueous solutions, and their excessive presence in fish and water leads to severe health problems, as demonstrated by the Minamata disease in Japan. Mercury ions significantly influence human mental and neurological functions by coordinating with thiol groups present in proteins,[4,5] while the interaction of copper ions with proteins and enzymes in the body can lead to gastrointestinal problems, osteoporosis, and various diseases including Alzheimer's disease.[6,7] Similarly, exposure to lead ions is linked with cardiovascular effects, increasing the blood pressure and raising hypertension rates of

[a] *Hebei Key Lab of Power Plant Flue Gas Multi-Pollutants Control, Department of Environmental Science and Engineering, North China Electric Power University, Baoding, 071003, P. R. China. E-mail: mlincepu@hotmail.com*
[b] *Key Laboratory of Bio-based Material Science and Technology of Ministry of Education, Material Science and Engineering College, Northeast Forestry University, Hexing Road 26, Harbin 150040, P. R. China. E-mail: chenzhijun@nefu.edu.cn*
[c] *Department of Chemistry, University of Bath, Bath, BA2 7AY, UK. E-mail: t.d.james@bath.ac.uk*
[d] *School of Chemistry and Chemical Engineering, Henan Normal University, Xinxiang 453007, P. R. China*

adults.[8,9] Therefore, the development of real-time and highly efficient sensors capable of detecting and removing metal ions is of great importance. Organic molecular probes,[10] biomolecules,[11] inorganic materials,[12] and a range of optical artificial systems have been used to construct functional materials for monitoring and removing heavy metal ions. These functional materials exhibit rapid recognition of heavy metal ions due to the mechanisms of photo-induced electron transfer (PeT), aggregation-induced emission (AIE), intramolecular charge transfer (ICT), Förster resonance energy transfer (FRET), inner filter effect (IFE), chelation-enhanced fluorescence (CHEF), and chelation quenched fluorescence (CHQF). Meanwhile, the porous structure and surface functional groups of these substrate materials play a critical role in the removal of heavy metal ions, leading to an excellent uptake ability for heavy metal ions. The specific mechanisms underlying detection and removal will be reviewed in the subsequent sections. Up to now, various techniques, including electrochemical analysis,[13,14] inductively coupled plasma mass spectrometry (ICP-MS),[15,16] atomic absorption spectroscopy,[17,18] and optical detection, have been explored for the monitoring of heavy metal ions.[10,19] Among the developed detection technologies, mass spectrometry (ICP-MS) and atomic absorption spectroscopy are considered as the main techniques for detecting heavy metal ions. However, these methods suffer from drawbacks such as high cost, complexity, and long analysis time, rendering them unsuitable for real-time online monitoring of heavy metal ions. Fluorescence detection methods, on the other hand, have emerged as a prominent approach for pollutant detection due to their ease of operation, excellent responsiveness, *in situ* monitoring capabilities, and high sensitivity.[20,21]

In fact, traditional materials suffer from high cost, poor stability, low sensitivity, long response time, and low removal efficiency. Therefore, it is imperative to develop novel materials and strategies with outstanding performance to overcome these challenges. Functional materials that integrate detection

Meng Li

Meng Li is now an associate professor at the North China Electric Power University. She obtained her BSc in 2011 (East China University of Science and Technology), and was a master combined with PhD student from 2011 to 2012 (with Prof. Weihong Zhu in China) and then worked with Prof. Tony D. James for a PhD degree at the University of Bath from October 2012 till July 2015. Her research interests comprise many aspects of supramolecular chemistry, environmental chemistry and materials chemistry, including pollutants recognition and materials fabrication for environmental remediation.

Quanyu Shi

Quanyu Shi studied at the School of Environmental and Chemical Engineering of Shanghai University of Electric Power from 2017 to 2021, majoring in Materials Chemistry. He graduated in 2021 with a Bachelor of Science degree in Materials Chemistry. From 2021 to now, he joined the School of Environmental Science and Engineering at North China Electric Power University as a master's student in the team led by Associate Professor Meng Li. His current research focuses on the integrated detection and removal of heavy metal ions in water using fluorescence multifunctional materials.

Ningxin Song

Ningxin Song studied at the School of Water Resources and Environmental Engineering of Nanyang Normal University from 2018 to 2022, majoring in Water Quality Science and Technology. She obtained her bachelor's degree from Nanyang Normal University in 2022. From 2022 to now, she joined the School of Environmental Science and Engineering at North China Electric Power University as a master's student in the team led by Associate Professor Meng Li. Her current research focuses on the integrated detection and removal of heavy metal ions using fluorescence carbon dots and gel materials.

Yumeng Xiao

Yumeng Xiao entered Hebei University of Science and Technology in 2018 to study environmental science (Sino-foreign cooperative education), and in 2022, she obtained a Bachelor of Science degree from Hebei University of Science and Technology and Australian Federal University. In the same year, she began to study for a master's degree in environmental engineering under the guidance of Associate Professor Meng Li from North China Electric Power University. At present, her main research direction is the control of pollutants in water alongside solar steam generation.

and removal capabilities offer significant advantages in the identification and elimination of heavy metal ions in water. Most conventional materials exhibit limited functionality in wastewater treatment, as they can only achieve singular detection or adsorption of heavy metal ions, thereby restricting their widespread application. The use of functional materials for the simultaneous detection and removal of pollutants in water not only reduces treatment costs but also improves material performance. When the adsorbent contains a probe, it can enhance the mechanical properties of the adsorbent and stabilize the probe, thereby improving water treatment efficiency. So far, significant research has been devoted to establishing various functional materials, including nanomaterials,[22,23] polymer materials,[24,25] porous materials,[26–28] and biomaterials,[29,30] for the treatment of heavy metal ions with low detection limits, high sensitivity, high selectivity, and large adsorption capacity. Each functional material possesses unique advantages and holds great potential in addressing the issue of heavy metal ion pollution in practical applications. Firstly, nanomaterials such as metal nanoprobes and photoluminescent carbon dots (CDs) have attracted attention in functional system development due to their unique electronic, magnetic, and optical properties.[31,32] Nanomaterials provide new strategies for constructing functional materials that can accurately, conveniently, and rapidly detect and remove heavy metal ions from water. Secondly, polymer materials possess abundant reactive groups and favorable structures, making them the preferred choice for constructing high performance chemical sensors. Undoubtedly, polymer probes exhibit outstanding recoverability, low cost, and advantages in green detection (the probe is linked with the polymer so it can be recycled and does not cause secondary contamination) when applied in real samples.[33,34] In addition, mesoporous silica, metal–organic frameworks (MOFs), and covalent organic frameworks (COFs), among other porous materials, have emerged as popular systems for the detection and removal of heavy metal ions due to their significant advantages, including extended π-conjugated frameworks, large surface areas, tunable functionality, and inherent porous structures.[35–38] Apart from the aforementioned three types of functional materials, biocompatible biomaterials have gained significant attention due to their multifunctionality and compatibility with living systems. Materials such as proteins and peptides exhibit unique advantages in constructing biosensors and medical devices.[39,40]

Currently, extensive developments have been made in functional materials to meet the growing demands of water pollution control. Considering the advantages of these functional materials, this review aims to summarize the latest progress in the detection and removal of heavy metal ions using different types of functional materials, including nanomaterials, polymers, porous materials, and biomaterials (Fig. 1). Additionally, the future prospects and challenges faced by these four material categories are discussed, with the hope of inspiring novel ideas in the

Lidong Wang

Lidong Wang received PhD degree in 2005 from North China Electric Power University, majoring in thermal power engineering. He was a postdoctoral fellow at Tsinghua University and a visiting scholar at the University of Illinois at Urbana-Champaign. Currently, he serves as the Dean in the School of Environmental Science and Engineering at North China Electric Power University. His main research focus is on pollution control, including heavy metal ions removal, flue gas desulfurization, denitrification, and carbon capture. He has hosted over 10 national-level research projects, and has published over 120 papers.

Zhijun Chen

Zhijun Chen was born in 1987 and received PhD degree in 2017 from the Max Planck Institute for Polymer Research, Germany, working on near-infrared sensitive materials under the supervision of Prof. Hans-Juergen Butt. Returned to China in 2017 and kicked off the independent research career at Northeast Forestry University as a full professor. Main research interest is sustainable photochemistry and optical materials from biomass sources, such as, photoluminescent materials, photothermal materials and photocatalytic materials. Published more than 100 papers with H-index of 31.

Tony D. James

Tony D. James is Professor at the University of Bath and Fellow of the Royal Society of Chemistry. He was a Royal Society University Research Fellow (1995–2000), Wolfson Research Merit Award holder (2017–2022) and was awarded the Daiwa-Adrian Prize (2013), the CASE Prize (2015), the MSMLG Czarnik Award (2018) and Frontiers in Chemistry Diversity Award (2020). His research interests include many aspects of Supramolecular chemistry, including probes for redox imbalance and theranostic systems. His h-index is 84 (Google Scholar) and he was listed by Clarivate as a Highly Cited Researcher in 2022.

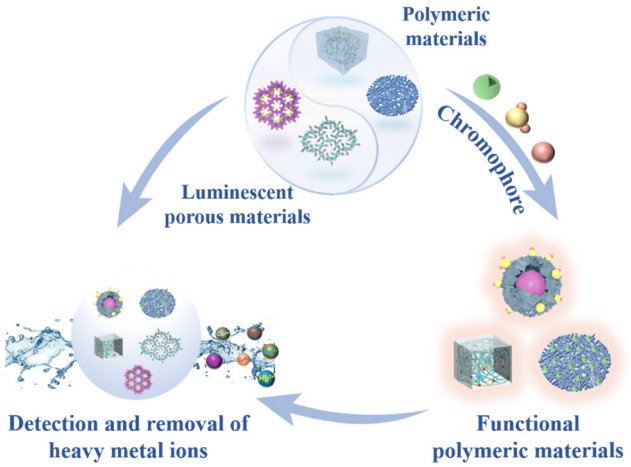

Fig. 1 Schematic diagram of functional materials fabrication and their applications for detection and removal of heavy metal ions.

detection and removal of heavy metal ions and fostering a better understanding of the future development in this research field.

2. Types of fluorescent probes for heavy metal ion sensing

There are several types of fluorescent probes for sensing heavy metal ions, such as molecular chromophores, nanomaterials, metal organic frameworks (MOFs), covalent organic frameworks (COFs), *etc.* Based on photophysical processes, fluorescent probes respond to heavy metal ions mainly through several signalling mechanisms including photo-induced electron transfer (PeT), aggregation induced emission (AIE), intramolecular charge transfer (ICT), Förster resonance energy transfer (FRET), inner-filter effect (IFE), chelation-enhanced fluorescence (CHEF), chelation-quenched fluorescence (CHQF) (Table 1).

2.1. Molecular chromophores

The addition of heavy metal ions into a solution containing a fluorescent probe frequently induces fluorescence quenching through mechanisms such as electron transfer, FRET, heavy atom effect, and spin–orbit coupling (Fig. 2). For example, Hg^{2+} ions can markedly quench the fluorescence of ligands. In 2017, John and co-workers designed a pyrene-amino mercapto thiadiazole fluorescent probe (Fig. 3a) for the detection of Hg^{2+} ions *via* a "turn-off" mode, exhibiting three emission peaks at 378, 388 and 397 nm.[41] Significant fluorescence quenching (96%) could be observed after binding with Hg^{2+} ions (Fig. 3b), while other metal ions (*e.g.* Pb^{2+} and Fe^{3+}) had little effect on the fluorescence intensity. This probe exhibited a good linear correlation with a wide range of Hg^{2+} concentrations, providing an impressive limit of detection (LOD) of 0.35 nM. The fluorescence quenching mechanism of this probe was attributed to the heavy atom effect induced by the Hg^{2+} ions.

The majority of organic fluorescent dyes or fluorophores exhibit strong fluorescence emissions in a solution state, whereas their fluorescence emission intensity is reduced when they are in a solid state or aggregated form.[42] However, Tang *et al.* observed that some flexible molecular systems exhibit weak emission in the solution phase but strong emission at high concentrations or when aggregated.[43] Such Aggregation-induced emission (AIE) molecular systems are now widely used as fluorescent sensors and optoelectronic materials.[44] In 2020, Feng and co-workers developed a non-planar tetraphenylethylene-functionalized salicylaldehyde Schiff base fluorescent probe (TPE–An–Py) (Fig. 3c) with aggregation-induced enhanced emission (AIEE) properties *via* a classical Knoevenagel condensation reaction.[45] Its fluorescence spectrum in tetrahydrofuran (THF) exhibited two emission bands at 477 nm and 598 nm corresponding to the enol and ketone forms, respectively. The probe can easily transfer from the enol form to the keto form *via* a photo-tautomerization process under photoexcitation *via* the excited-state intramolecular proton transfer (ESIPT). Based on a ligand-induced complexation mechanism, coordination between Cu^{2+} and the nitrogen and oxygen atoms in the Schiff base result a selective off response of TPE–An–Py towards Cu^{2+} in a mixture of THF and water (Fig. 3d). The detection limit of the probe for Cu^{2+} was determined to be 2.36×10^{-7} M based on the "turn-off" fluorescence detection. Meanwhile, this probe also provides a convenient "naked eye" detection method for Cu^{2+} ions, demonstrating its promising potential as a sensitive and selective sensing platform for heavy metal ions, which pave the way for the development of novel fluorescent probes with tunable properties for a wide range of applications in chemical and biological sensing.

Nevertheless, since fluorescent sensors based on a quenching mechanism may provide false signals, they are less practically applicable. Compared with turn-off sensors, turn-on sensors exhibit higher accuracy in detecting heavy metal ions. In 2019, Patra and co-workers designed a bis-Schiff base chemosensor incorporating triazole moieties, which exhibits colorimetric and fluorescent response towards Pb^{2+} and Cu^{2+} ions (Fig. 4a) *via* a "turn-on" mechanism.[46] The free triazole probe exhibited a weak fluorescence emission at 440 nm, which was attributed to a non-radiative PeT process from the nitrogen to the excited fluorophore. In the presence of Cu^{2+} or Pb^{2+} ions, a remarkable

Table 1 Examples of chromophores for the detection of heavy metal ions

Chromophores	Signal	Mechanism	Analytes	LOD (M)	Ref.
Pyrene-amino mercaptothiadiazole	Fluorescence quenching	Heavy atom effect	Hg^{2+}	0.35×10^{-9}	41
TPE–An–Py	Fluorescence quenching	CHQF	Cu^{2+}	2.36×10^{-7}	45
Schiff base	Fluorescence increase	ICT	Pb^{2+}	1.24×10^{-3}	46
Tmbipe	Fluorescence increase	CHEF	Hg^{2+}, $MeHg^{+}$	6.30×10^{-10}	47
H_2Pc, ZnPor	Ratiometric response	FRET	Pb^{2+}	4.10×10^{-9}	49
Tetraphenylene, Rho	Ratiometric response	DTBET	Hg^{2+}	1.50×10^{-9}	50

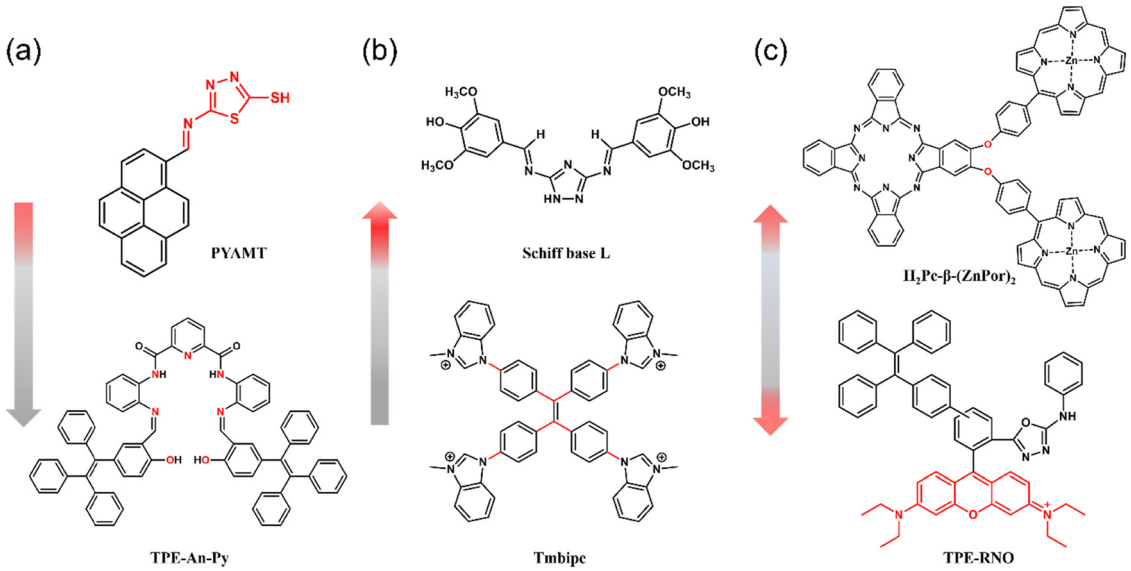

Fig. 2 Chromophores with different fluorescence response for the detection of heavy metal ions. (a) Fluorescence quenching. (b) Fluorescence enhancement (c) ratiometric sensing.

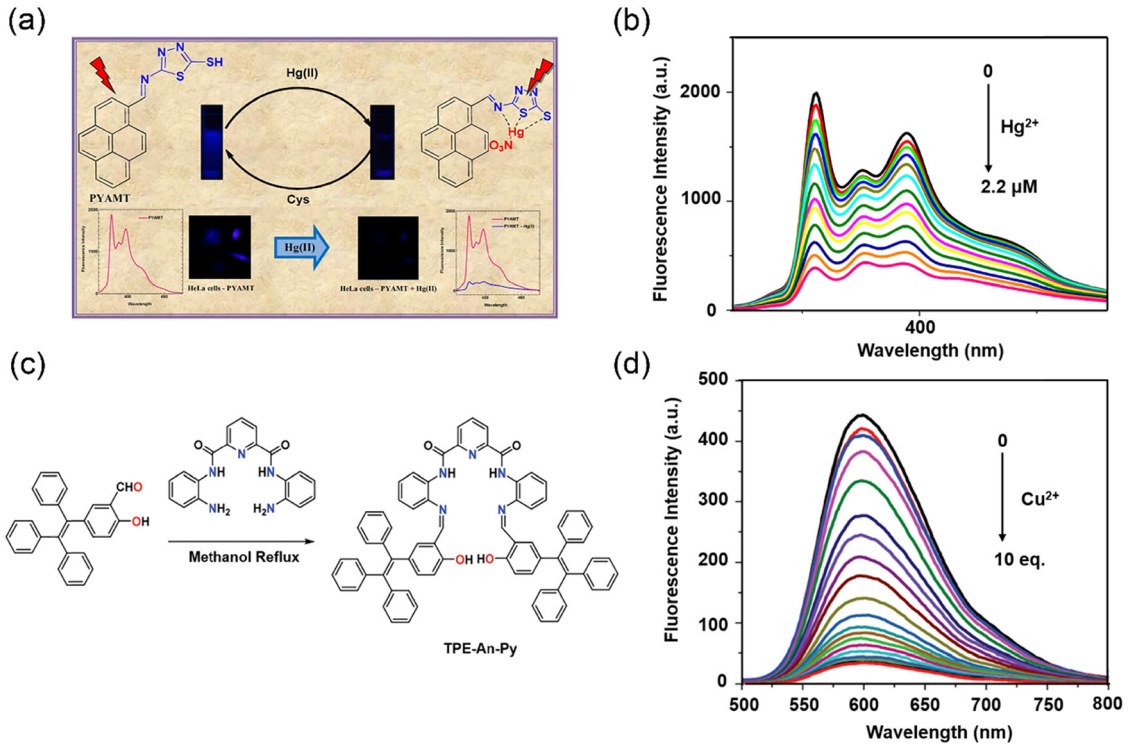

Fig. 3 The synthesis of "turn-off" fluorescent probes and their fluorescence spectra for detecting heavy metal ions. (a) Pyrene-based fluorescent probe for detection of Hg^{2+} ions with turn-off response. (b) Fluorescence spectra of PYAMT in the presence of Hg^{2+}. Reproduced from ref. 41 with permission from Elsevier B.V. Copyright 2017. (c) Synthetic route to probe TPE–An–Py. (d) Fluorescence response of TPE–An–Py on addition of Cu^{2+}. Reproduced from ref. 45 with permission from Royal Society of Chemistry. Copyright 2020.

amplification of fluorescence intensity by approximately 15-fold and 17-fold, respectively, was observed at 440 nm (Fig. 4b), accompanied by a blue shift of the emission wavelength to 412 nm. In contrast, no significant spectral changes were observed upon the addition of other metal ions. The LOD for Pb^{2+} and Cu^{2+} ions were determined as 0.99 mM and 1.24 mM, respectively. The underlying mechanism for the observed enhancement was attributed to the coordination of Pb^{2+} or Cu^{2+}

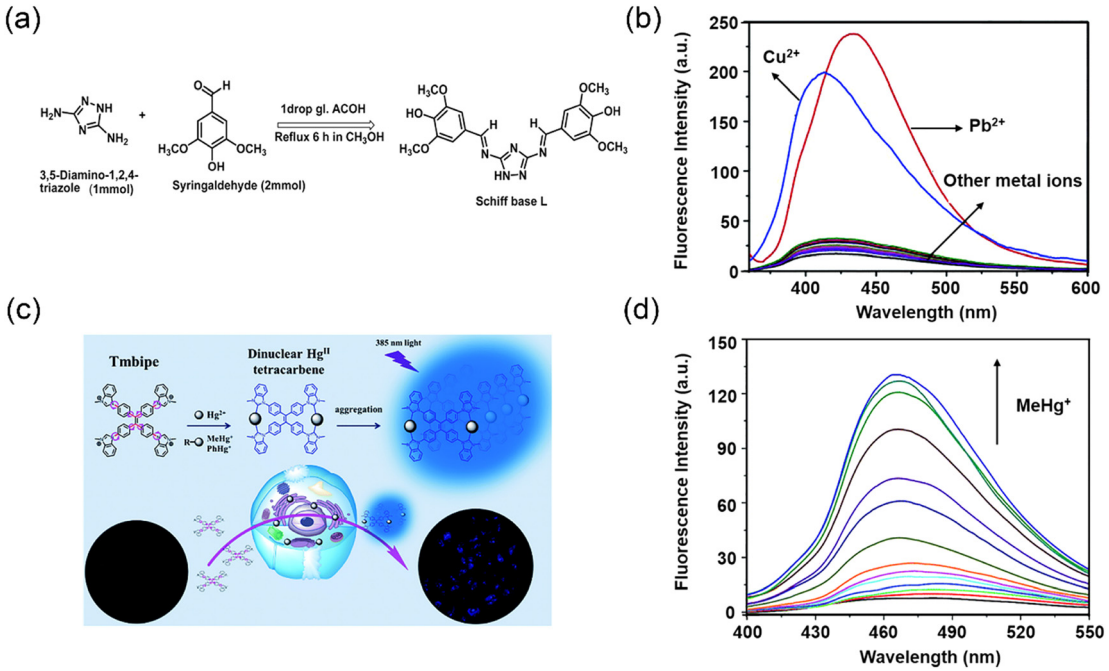

Fig. 4 The synthesis of "turn-on" fluorescent probes and their fluorescence spectra for detecting heavy metal ions. (a) Synthesis of fluorescence probe L. (b) Fluorescence response of L after adding different metal ions. Reproduced from ref. 46 with permission from Royal Society of Chemistry. Copyright 2019. (c) Structure of Tmbipe and its application. (d) Fluorescence spectra of the Tmbipe probe in presence of $MeHg^+$. Reproduced from ref. 47 with permission from Royal Society of Chemistry. Copyright 2019.

with the triazole moieties and imine unit, which impedes the PeT process and reinforce the ICT process. Subsequently, Yuan and co-workers reported a benzimidazole-modified 1,1,2,2-tetrakis[4-(3-methyl-1*H*-benzimidazol-1-yl)phenyl]ethylene tetraiodide (Tmbipe) probe (Fig. 4c) for the detection of Hg^{2+}.[47] The probe exhibits negligible fluorescence emission in aqueous media. Which was attributed to the C–C bonds between phenyl rings and C=C bonds and the C–N bonds between phenyl rings and benzimidazoles exhibiting high rotational freedom, which diminished the molecular planarity, while concurrently increasing the possibility of radiationless relaxation. As such the probe exhibited significant fluorescence enhancements with Hg^{2+} and organic mercury ($MeHg^+$ and $PhHg^+$) (Fig. 4d). It was proposed that Hg^{2+} can coordinate with two benzimidazole units to form a binuclear tetracarbene Hg^{2+} complex, which is similar to the reported Ag^+ or Au^+ tetracarbene complexes.[48] Therefore, free rotation is restricted due to formation of a closed macrocyclic structure, which triggers the fluorescence enhancement. Dynamic light scattering (DLS) results indicated that the average size of the probe in solution increased dramatically from 1.3 nm to 1000 nm after the addition of Hg^{2+}, confirming the formation of large aggregates.

The dual-channel signal based on the FRET effect provides more accurate and stable response when compared to single-channel signaling. Jiang and co-workers designed a phthalocyanine–porphyrin hetero-triad H_2Pc-β-$(ZnPor)_2$ probe for the ratiometric fluorescence detection of Pb^{2+} ions (Fig. 5a).[49] The ratiometric fluorescence response relied on the coupled FRET and a metal-chelating induced fluorescence quenching. Specifically, the probe exhibited highly efficient intramolecular FRET from the two zinc–porphyrin (ZnPor) units to the metal-free phthalocyanine (H_2Pc) unit. Selective binding of Pb^{2+} to H_2Pc effectively quenched the emission of the phthalocyanine unit, and the emission of the ZnPor units recovered due to suppression of the intramolecular FRET process, resulting in an obvious ratiometric fluorescent response (Fig. 5b). The addition of Pb^{2+} resulted in a significant 82-fold increase in the emission intensity ratio of ZnPor and H_2Pc, and a good linear relationship to Pb^{2+} concentrations over a range from 0–2.0 μM was observed, resulting in a LOD value of 4.1 nM that was not affected by other heavy metal ions. Tang and co-workers devised a dark through-bond energy transfer (DTBET) strategy for the development of high-performance ratiometric Hg^{2+} sensors (Fig. 5c).[50] The system used a tetraphenylene (TPE) derivative with AIE characteristics as the dark donor to eliminate the leakage of donor emission. Energy transfer from the TPE derivative (dark donor) to the rhodamine unit (acceptor) proceeded with an energy transfer efficiency (ETE) of 99%. The through-bond energy transfer (TBET) mechanism was used due to the reduced sensitivity to spectral overlap than FRET, allowing for greater flexibility in the design of the system with large pseudo-Stokes shifts. The addition of Hg^{2+} results in two distinct effects: (i) the generation of a rhodamine core, leading to increased PL at 595 nm and decreased PL intensity of the TPE moiety due to rapid and efficient TBET processes; (ii) the reduction of sensor aggregation, resulting in a fluorescence decrease of the TPE unit (Fig. 5d). The sensor exhibited an ultra-high ratiometric enhancement and a very low detection limit of 0.3 ppb. Therefore,

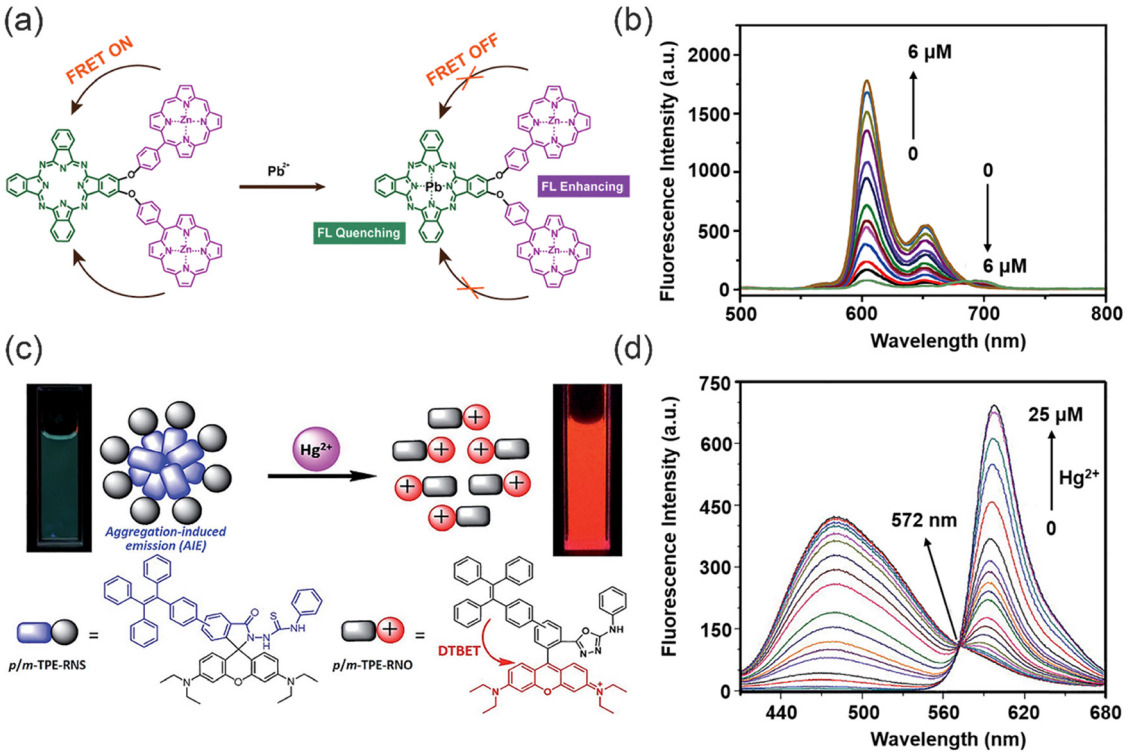

Fig. 5 The synthesis of "ratiometric" fluorescent probes and their fluorescence spectra for detecting heavy metal ions. (a) The sensing mechanism of ratiometric probe for Pb^{2+}. (b) fluorescence spectra of triad 1 upon addition of Pb^{2+}. Reproduced from ref. 49 with permission from Elsevier Ltd. Copyright 2019. (c) The sensing mechanism of p/m-TPE–RNS for Hg^{2+}. (d) Fluorescence spectra of 10 mM m-TPE–RNS under different concentrations of Hg^{2+}. Reproduced from ref. 50 with permission from Royal Society of Chemistry. Copyright 2017.

the combination of AIE and DTBET is a good design strategy for the development of high-performance sensors.

To improve the removal efficiency of heavy metal ions, molecular fluorescent probes have been incorporated into polymeric and porous materials. Such integration enables the simultaneous detection and removal of heavy metal ions, providing a comprehensive solution for environmental monitoring and remediation.

2.2. Nanomaterials

Nanomaterials are substances whose physical dimensions are within the nanoscale range, typically ranging from 1 to 100 nanometers, or those that possess a nanoscale internal structure or surface morphology. In general, common nanomaterials used in sensing heavy metal cations include metal nano materials,[51,52] nano carbon materials,[53,54] and nanofiber materials.[55,56] Such nanomaterials exhibit special properties including surface effects, small size effects, quantum effects, and macro quantum tunnel effects.[57] These properties contribute to their high sensitivity and selectivity. Consequently, a plethora of nanomaterials have been used for the purpose of detecting heavy metal ions in wastewater.[58,59]

2.2.1. Metal nanomaterials. Metallic nanoparticles have gained considerable attention as fluorophores due to their size-dependent electronic transitions and high fluorescence emission intensity. Amongst which, gold and silver nanoparticles have emerged as promising sensing platforms, owing to their unique interaction with heavy metal ions, such as the D_{10}–D_{10} interaction between gold nanoparticles and Hg^{2+},[60–64] which results in excellent performance for the detection of heavy metal ions.[65] Zhang and co-workers constructed highly luminescent gold–thiol nanocrystals (SMBD@AuNCs) for Hg^{2+} detection using a simple one-pot method with 2-mercaptobenzimidazole-5-sulfonic acid sodium salt (SMBD) (Fig. 6a).[66] The 2-mercaptobenzimidazole-5-sulfonic acid sodium salt contains a thiol group, an imidazole ring and a sulfonate group attached to an aromatic ring, which can be used as an effective stabilizer and reducing agent. The fluorescence of SMBD@AuNCs was rapidly and significantly quenched after binding with Hg^{2+} (Fig. 6b). Hg^{2+} resulted in the fluorescence quenching of AuNCs due to the formation of a metallophilic bond between the $5d_{10}$ centers of Hg^{2+} and Au^{+} with high specificity and affinity. The Hg–Au amalgam formed by the enhanced interaction between Hg^{2+} and Au^{+}, significantly quenches the fluorescent AuNCs. The detection limit for Hg^{2+} was 0.5 nM with a linear range from 4.0 nM to 20.0 μM (R^2 = 0.999), enabling the detection of trace amounts of Hg^{2+} in real water samples. Similarly, Liu and co-workers designed a colorimetric probe for Hg^{2+} with high sensitivity and selectivity employing gold nanoparticles (AuNPs) as the sensing moiety (Fig. 6c).[67] The sensing mechanism relies on the formation and aggregation of Au–Hg alloy, leading to a distinct tri-color transition from red (representing AuNPs) to sandy beige (indicating the formation of Au–Hg alloy) and finally to celandine green (corresponding to larger Au–Hg alloy) (Fig. 6d). Specifically, in the presence of

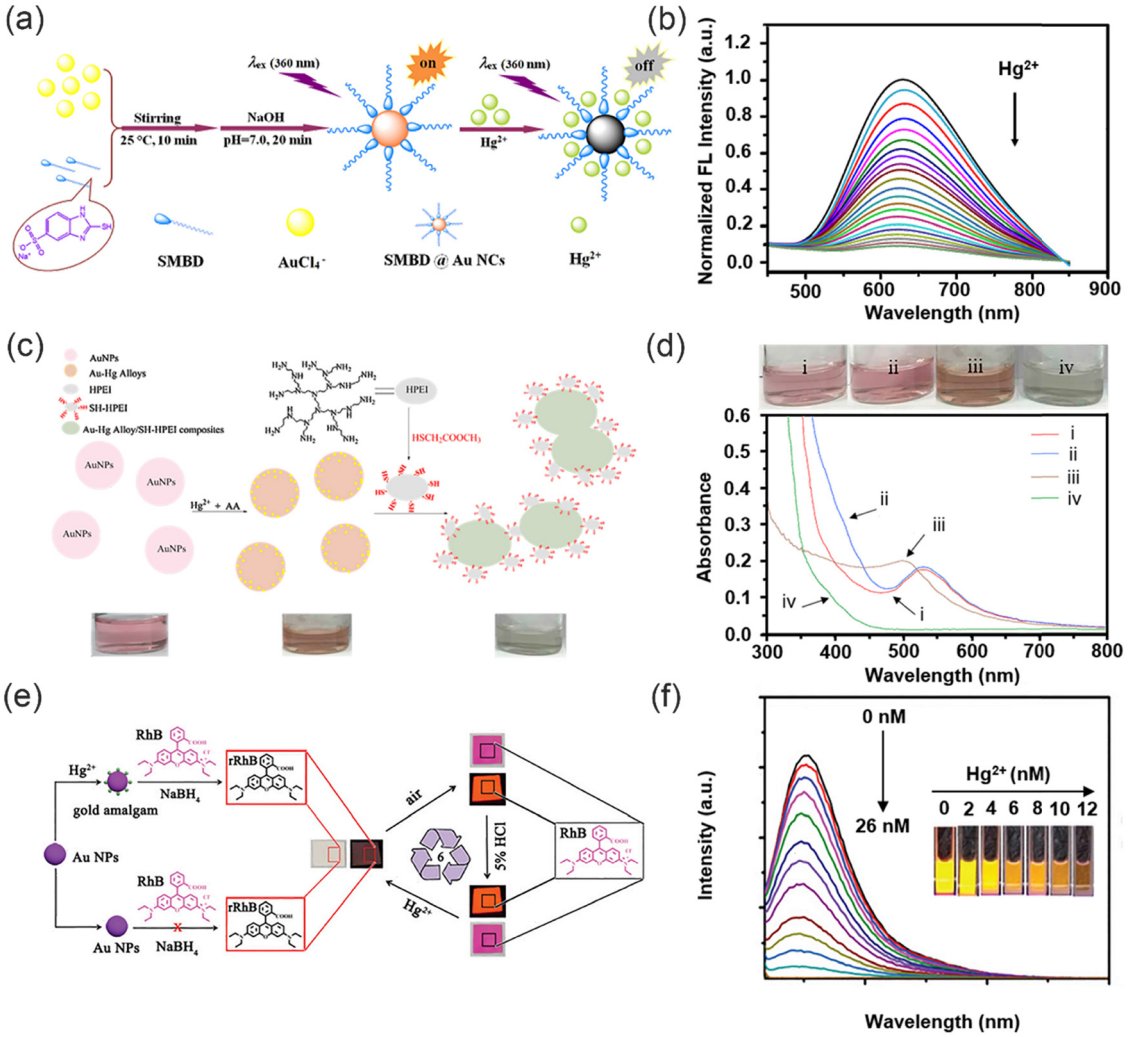

Fig. 6 The synthesis of metal nanoprobes and their sensing mechanisms for heavy metal ions. (a) The synthesis of SMBD@AuNCs. (b) Fluorescence response of SMBD@AuNCs under different concentrations of Hg^{2+}. Reproduced from ref. 66 with permission from Elsevier B.V. Copyright 2019. (c) Synthesis of SH-HPEI and the fluorescence response to Hg^{2+}. (d) Photographs and UV-vis absorption spectra of AuNPs. Reproduced from ref. 67 with permission from Elsevier B.V. Copyright 2017. (e) The sensing mechanism of fluorescent probes for detection of Hg^{2+}. (f) The fluorescence response of RhB with AuNPs and $NaBH_4$ under different concentrations of Hg^{2+}. Reproduced from ref. 68 with permission from Royal Society of Chemistry. Copyright 2017.

ascorbic acid, Hg^{2+} undergoes reduction to Hg^0, which subsequently gets deposited onto the surface of AuNPs, resulting in the formation of Hg–Au alloys and a distinct color change from red to sandy brown. In contrast to conventional colorimetric assays that typically exhibit a single-color change from red to blue or purple, this assay demonstrates exceptional selectivity for Hg^{2+} detection. The possibility of encountering identical three-color transitions induced by interfering agents is remarkably low, rendering this assay highly selective for Hg^{2+} sensing. The detection limit of this colorimetric sensor towards Hg^{2+} was 8.76×10^{-9} M with a good linearity over a range from 8.76×10^{-9} to 1.27×10^{-4} M. Notably, the introduction of multi-mercapto-functionalized hyperbranched polyethyleneimine, possessing abundant thiol and amine groups, to the solution induces the aggregation of Hg–Au alloys, leading to the formation of larger Hg–Au alloys and a color transition from sandy yellow to green. This unique colorimetric response enables the sensitive and selective detection of Hg^{2+}. Due to the three colour changes in the gold nanoparticle system, this sensing platform exhibits promising potential for high-performance detection of Hg^{2+} with exceptional sensitivity and selectivity, offering new opportunities for environmental monitoring and analytical applications.

Wang and co-workers used AuNPs as chemosensors for the dual signal amplification detection of Hg^{2+} (Fig. 6e).[68] This simple method presents some notable advantages, including simple synthesis, rapid response, exceptional selectivity, and high sensitivity. The proposed system relies on the formation of gold amalgam and a gold amalgam-based reaction involving rhodamine B (RhB) and $NaBH_4$, which exhibits fluorescence and colorimetric sensing functionalities. RhB was strategically selected as the visible signaling reporter due to its remarkable attributes, including long-wavelength absorption and emission,

high absorption coefficient, exceptional quantum efficiency, and superior photostability. Notably, the strong and specific D_{10}–D_{10} metallophilic interaction between Au^{+} and Hg^{2+} facilitates the catalytic reduction of RhB by the as-formed gold amalgam, leading to simultaneous changes in fluorescence and color of RhB (Fig. 6f), thus enabling dual signal amplification. Remarkably, the reduction product of RhB can be readily oxidized to regenerate RhB in air, allowing for repeatable and reusable utilization of the prepared sensor. To sum up, due to the specific interaction between metal nanomaterials and heavy metal ions, heavy metal ions can be identified precisely and sensitively in solution. Therefore, metal nanoparticles are promising practical tools for heavy metal ions detection.

2.2.2. Carbon dots. Carbon dots (CDs) are quasi-spherical particles with a diameter of less than 10 nm that can be prepared by simple methods,[69–72] and exhibit significant potential for wastewater treatment due to their adventitious properties, such as tunable photoluminescence (PL),[73–75] eco-friendliness, low bio-toxicity and multiple active sites.[76,77] Moreover, the intricate interplay of complexation and electron transfer phenomena between the surface-active functional groups and the graphite-like core of CDs with heavy metal ions results in the selective quenching of fluorescence emission from CDs.[78,79] This phenomenon arises from the intricate coordination chemistry and redox interactions that occur at the interface of CDs and heavy metal ions, leading to the modulated emission behavior of CDs. This elucidates the multifaceted nature of CDs and their potential for tailored sensing and detection applications in the realm of heavy metal ion detection.

Currently, CDs can be synthesized using two strategies, a top-down or bottom-up approach (Fig. 7).[80] The top-down method involves the fragmentation of a wider range of carbon-based materials (graphite, carbon black, graphene oxide, *etc.*) into quantum-sized particles by chemical oxidation or electrical discharge, laser ablation, and acid exfoliation under harsh synthetic conditions. In 2021, Carbone and co-workers synthesized nitrogen-doped carbon quantum dots (N-CQDs) (Fig. 8a) by a top-down method using fullerene as the raw material.[81] Since the opening of the fullerene rings requires a mixture of hydrogen peroxide (H_2O_2) and ammonia (NH_4OH), which generates oxygenated and nitrogenated functional groups. The process of hydroxyl-radical-induced opening of fullerene results in the modification of the surface of the resulting carbon quantum dots (CQDs) with various functional groups including hydroxyl (–C–OH), carboxyl (–CHO, –COOH), ether and/or epoxy (–C–O–C–), amine (–C–NH_2), and amide (–CO–NH_x, x = 1, 2) moieties. XPS and Fourier transform infrared spectroscopy (FTIR) confirmed that the surface of the synthesized carbon dots was rich in reactive groups (hydroxyl, carboxyl and amino groups), which could provide sufficient reactive sites for heavy metal ion chelation. When Cu^{2+} and Cr^{3+} are added, the fluorescence intensity of the CDs was reduced by 44% and 60%, respectively (Fig. 8b). However, the high price of raw materials, complex preparation process, and relatively low yield results in a the high cost for the preparation of these CDs.[82] Therefore, alternative approaches are required to improve the synthetic methods towards such CDs. The top-down methods for the synthesis of carbon dots typically require harsh conditions and high costs. In most cases, this method of synthesizing CDs is challenging and time-consuming.

Compared to top-down strategies, bottom-up approaches have significant advantages such as mild reaction conditions, rich carbon resources and better material morphology.[83] This method is also known to be a green method of synthesizing CDs. Since, many renewable green resources are used to prepare CDs such as lemons, honey, flowers, and silk.[84] Bottom-up approaches for the preparation of CDs include small molecule condensation, cross-linking or carbonization by hydrothermal methods, pyrolysis and microwave-assisted synthesis.[85–87] These methods are simple, low cost, and eco-friendly, resulting in the green synthesis of CDs. In 2019, Liu and co-workers synthesized fully water-soluble nitrogen-doped carbon dots (N-CDs) using barley as the carbon source and ethylenediamine as the nitrogen source for the detection of Hg^{2+} (Fig. 8c).[88] XPS and FTIR spectra confirmed that N-CDs carry a large number of

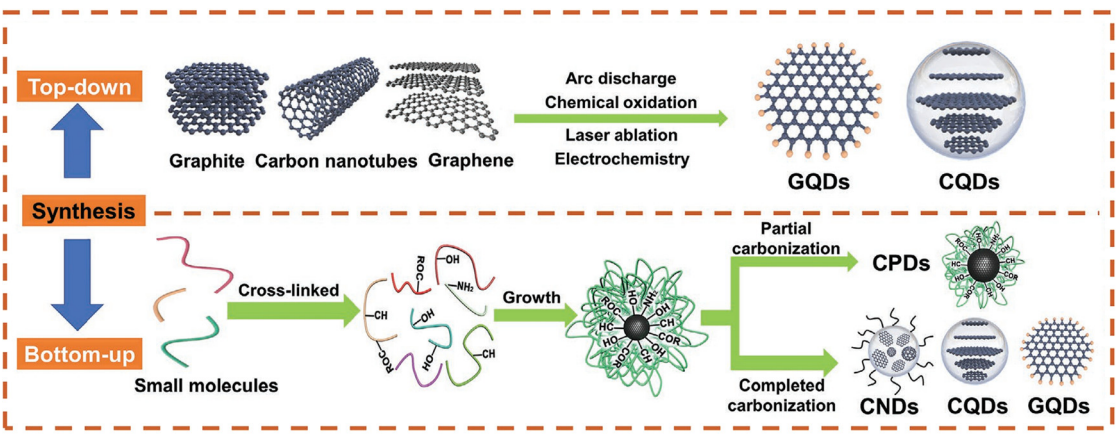

Fig. 7 Schematic illustration of the synthesis of CDs *via* top-down and bottom-up methods. Reproduced from ref. 80 with permission from Wiley-VCH. Copyright 2021.

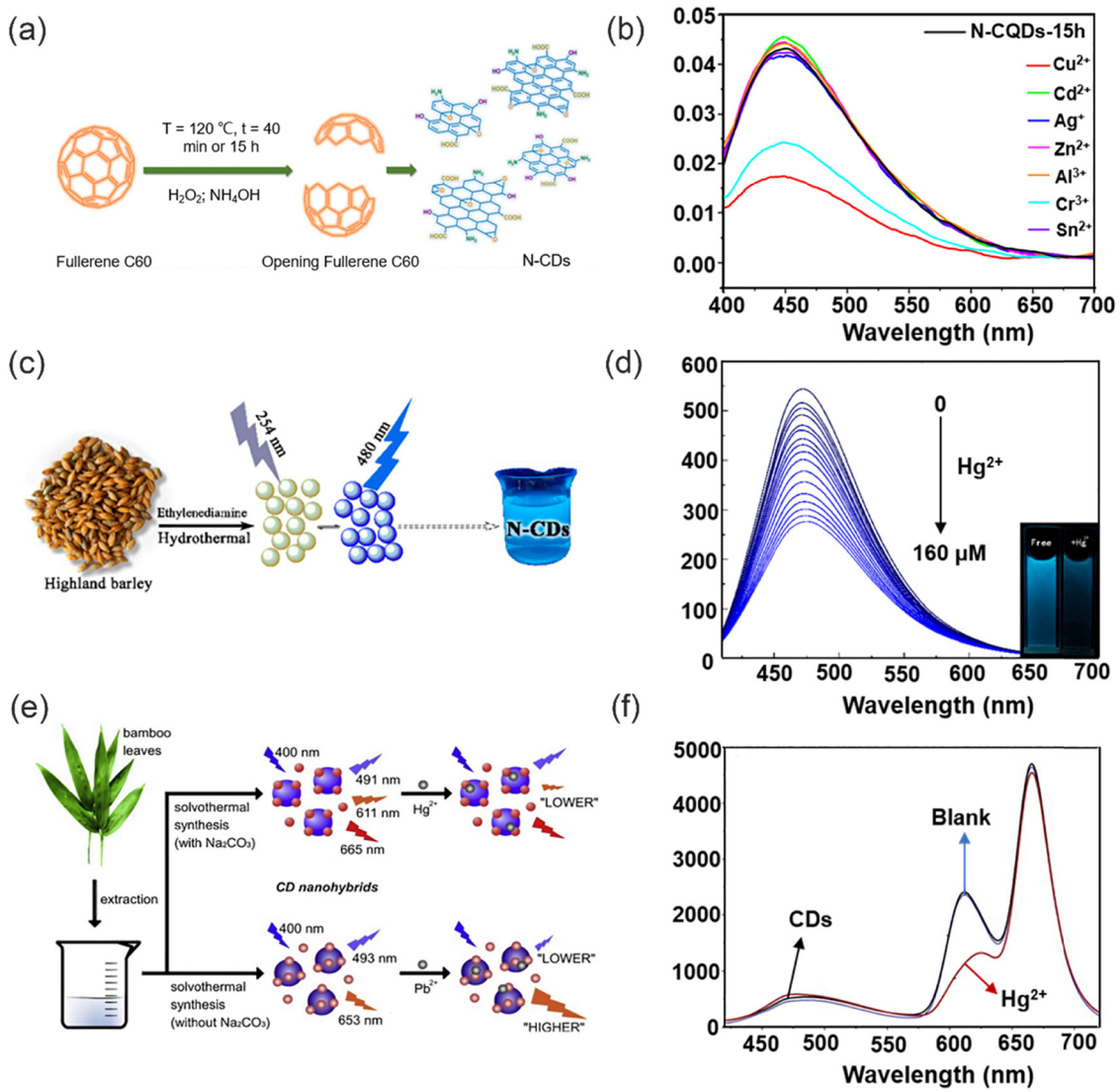

Fig. 8 The synthesis of CDs *via* top-down (or bottom-up) and their fluorescence response to heavy metal ions. (a) Preparation of fluorescent N-CQDs. (b) The fluorescence spectra of N-CQDs-15 h in the presence of different metal ions. Reproduced from ref. 81 with permission from Multidisciplinary Digital Publishing Institute Copyright 2021. (c) The preparation of the N-CDs. (d) The fluorescence response of the N-CDs under different concentrations of Hg^{2+}. Reproduced from ref. 88 with permission from Multidisciplinary Digital Publishing Institute. Copyright 2019. (e) Synthesis of dual- and three-emission CD nanohybrids for ratiometric fluorescent sensing of Pb^{2+} and Hg^{2+}, respectively. (f) Fluorescence spectra of the three-emission CD nanohybrids before and after its application for the analysis of a blank sample. Reproduced from ref. 89 with permission from Elsevier B.V. Copyright 2019.

reactive hydrophilic groups (oxygen and nitrogen containing functional groups) on their surface. The remarkable fluorescence quenching observed in the N-CDs is attributed to the robust chelating ability of Hg^{2+} ions towards the carboxylic functional groups on the surface of N-CDs, as depicted in Fig. 8d. This interaction leads to the formation of a non-fluorescent complex, facilitating non-radiative electron/hole annihilation through an efficient electron transfer process. Therefore, the fluorescence of N-CDs is effectively quenched through a static quenching mechanism. In addition, the N-CDs are environmentally friendly since the N-CDs were prepared using natural biomass as the raw materials. Similarly, Zhang and co-workers have successfully developed two new dual-emission and triple-emission CD nanohybrid ratiometric fluorescent nanosensors for the simple, sensitive and specific detection of Pb^{2+} and Hg^{2+} in complex environmental water samples, respectively (Fig. 8e).[89] These two novel CD hybrids were prepared by solvent heat treatment of the same bamboo leaf extract. This method is characterized by its simplicity, cost-effectiveness, environmental sustainability, and practicality, as it circumvents the need for post-modification of CDs or co-incorporation with other fluorescent probes. Notably, these newly developed nanosensors exhibit built-in correction capabilities owing to their dual emission behavior, enabling detection limits as low as 0.14 nM and 0.22 nM for Pb^{2+} and Hg^{2+} respectively (Fig. 8f). The system was particularly sensitive for the selective detection

of these analyte ions, indicating the unlimited possibilities of the nano-probe in chemical analysis of real samples.

In order to meet the demand for both detection and removal of heavy metal ions, researchers have explored the integration of nanomaterials into polymer matrices. The incorporation of nanomaterials within polymer matrices results in excellent functional materials capable of the simultaneous detection and removal of heavy metal ions.

2.3. DNA or RNA Biomaterials

The interaction of heavy metal ions with DNA, RNA and other biomolecules provides biomaterials with a remarkable advantage in terms of selectivity, thus facilitating the recognition and elimination of heavy metal ions. Specific aptamer-target interactions (T–Hg^{2+}–T) in the presence of Hg^{2+} and aptamer make biomaterials functional for the detection of Hg^{2+}. Wu and co-workers developed a Hg^{2+} sensing platform based on T–Hg^{2+}–T pairing using a single-channel recording technique for the detection of Hg^{2+}.[90] The presence of Hg^{2+} can be confirmed at around 7 nM within 30 min. The sensor is manufactured from off-the-shelf materials, does not require synthesis, purification, or probe fabrication processes, and is highly selective for Hg^{2+} without interference from other metal ions. This sensing strategy opens new possibilities for the detection of many types of analytes that have specific interactions with DNA molecules.

In recent years, significant advancements have been made in enhancing the sensitivity of sensors for Hg^{2+}. In 2017, Chen and co-workers reported a versatile and sensitive colorimetric sensor for Hg^{2+} based on aptamer-target specific binding and target-mediated growth of AuNPs.[91] T bases were used to detect Hg^{2+} by T–Hg^{2+}–T coordination (Fig. 9a) and a detection limit of 9.6×10^{-9} M (Fig. 9b) was determined, different lengths of aptamer effected the sensitivity of Hg^{2+} detection. Starting with the 15-mer aptamer, the DNA sequences were extended and truncated to produce 25-, 59- and 8-mer (8T) sequences, and it was found that the detection performance of the 25-mer and 59-mer aptamers was greater than that of the 15-mer aptamer. In the presence of Hg^{2+}, T–Hg^{2+}–T coordination makes the T-base sequence detach from the AuNP surface, while the additional A base sequence remains adsorbed on the AuNP surface, thus differences in the number of DNA strands adsorbed may lead to morphological changes in the grown AuNP. This also indicates that the increased sensitivity due to prolonging aptamer strands can result in enhanced LOD. In 2021, Liu and co-workers developed a simple method to covalently incorporate unmodified DNA oligonucleotides to hydrogel nanoparticles and monoliths using A_5 as an anchoring block (Fig. 9c).[92] Various functional DNA sequences were ligated by designing DNA containing A_5 blocks. The DNA was folded into a hairpin shape after Hg^{2+} mediated T–Hg^{2+}–T formation. The DNA functionalized hydrogels were utilized to detect Hg^{2+} ions, demonstrating a remarkable detection limit of 10 nM (Fig. 9d). The thymine interaction with Hg^{2+} is particularly important for sensing applications. All the methods based on this interaction show excellent selectivity over other

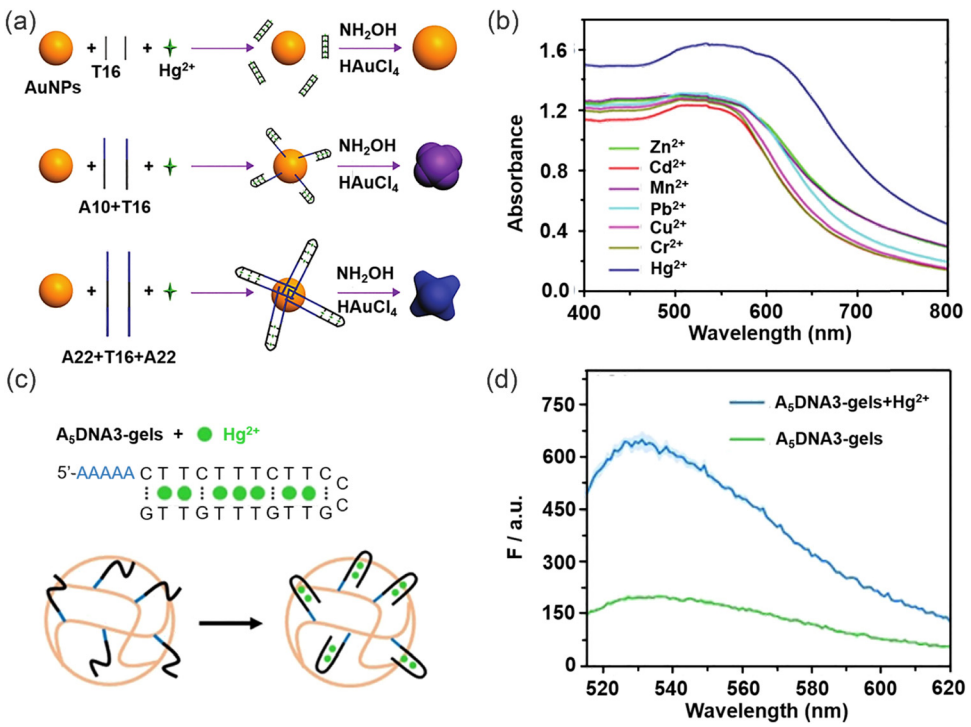

Fig. 9 The specific receptors with strong metal binding ability of DNA or RNA biomaterials to facilitate the detection of Hg^{2+}. (a) The sensing strategy for the colorimetric detection of Hg^{2+} based on the growth of AuNPs induced by different amounts of bases (adenine and thymine). (b) Absorption spectra of AuNPs grown in the presence of Hg^{2+} and other interfering heavy metal ions. Reproduced from ref. 91 with permission from Wiley-VCH. Copyright 2017. (c) The sequence of the A_5DNA3 and Hg^{2+} binding to A_5DNA3 containing hydrogel nanoparticles. (d) Fluorescence spectra of Hg^{2+} binding to A_5DNA3 hydrogels. Reproduced from ref. 92 with permission from Wiley-VCH. Copyright 2021.

heavy-metal ions due to the high specificity and strength of the complex formed with Hg^{2+}, which ensures that such biomaterials are ideal for heavy metal ions sensing. A similar approach was used in 2022 to fabricate supramolecular polymers with high efficiency for the detection and removal of Ag^{+} ions.[93] Through, the incorporation of functional macrocycles and fluorescent molecules into the supramolecular polymers, an ideal material for detection and removal applications could be developed, offering new avenues for pollutant monitoring and environmental remediation. This innovative strategy holds great potential in the field of pollution detection and environmental management.

3. Chromophore incorporated Polymeric Materials

Polymeric sensing materials, consisting of fluorescent probes and a hydrophilic polymer matrix, have drawn significant attention due to their remarkable ion-specific selectivity and exceptional sensitivity.[10,94] A hydrophilic polymer is preferred, since while conventional hydrophobic polymers are more effective for heavy metal ion removal, they exhibit limited detection ability in waste water. While, fluorescent probes are difficult to remove from the sample for recycling, which limits their application in real water samples or wastewater.[95] To tackle these problems, hydrophilic functional polymer materials with good sensing and removal abilities have been constructed (Fig. 10). Notably, the advantages of polymer-based functional systems are as follows: (i) additional adventitious properties are provided by functional polymer materials (*e.g.* good mechanical properties, pore size structure, hydrophilicity and reusability, *etc.*); (ii) larger reactive regions and more binding sites available on functional polymers;[96] (iii) the loading and encapsulation of fluorescent materials using polymers can improve the stability and enable them to be used for a variety of environmental applications; (iv) some polymers can be designed to be degradable, which allows them to break down into harmless substances in the environment, reducing their impact. In addition, the mechanical properties of polymers can also impart fluorescent materials with good processability. It should be noted that the advantages of polymer-based functional systems are not limited to the polymers themselves. In many cases, these systems can be carefully designed to possess additional functionalities, such as optical, electrical, or magnetic properties. As a result, polymer-based functional systems have broad applications in various fields, including environmental remediation, and also energy storage.

3.1. Membrane-based materials

Membrane filtration is an effective separation technique that uses the selective permeability of a membrane under the influence of a driving force, such as pressure, to effectively separate substrates. Polymeric membranes exhibit great promise for heavy metal ion removal due to their ease of processing, high mechanical strength and acceptable separation performance. Nevertheless, while conventional polymeric membranes exhibit good retention ability for heavy metal ions, the ability to identify heavy metal ions requires improvement. As such polymer membranes can be modified to have the ability to both identify and remove heavy metal ions. The hydrophilicity and pore size of the modified polymer membrane will also be modified, potentially enhancing the retention capacity of the polymer membrane for heavy metal ions (Fig. 11). In addition, the polymer structure can provide a good carrier for chromophores, which enhances the stability and reusability of the chromophores.

Chuang and co-workers designed a novel functional membrane material for the detection and removal of Cr(VI) (Fig. 12a).[97] Phthalocyanine (Pc) derivatives and hyperbranched polyamidoamines (HPAMAM) were coupled to polytetrafluoroethylene (PTFE) membranes modified with furan groups *via* the Diels–Alder (DA) reaction. Fluorescence quenching occurs when Pc forms chelates with specific heavy metal ions (Fig. 12b). To mitigate the rapidly flow of detected heavy metal ions, hyperbranched poly(amidomethylamine) (PAMAM) can effectively sequester heavy metal ions through the formation of chelates. The intricate dendritic architecture of PAMAM, functionalized by numerous primary and tertiary amine groups, enables it to retain heavy metal ions through chelation.[58,98–102] In addition, after modification by HPAMAM and Pc, the surface pore structure of the membrane is partially filled with a thick polymer layer, resulting in the average pore size of the membrane being reduced from 2.3 μm to 1.3 μm. Significantly, the 145.2 ± 0.17° contact angle of the extremely hydrophobic neat PTFE membrane was decreased to 57.7 ± 0.80° by the hydrophilic polymer HPAMAM. The membrane surface pore size was decreased by the polymer layer following HPAMAM/Pc modification, and the decreased hydrophobicity improved water

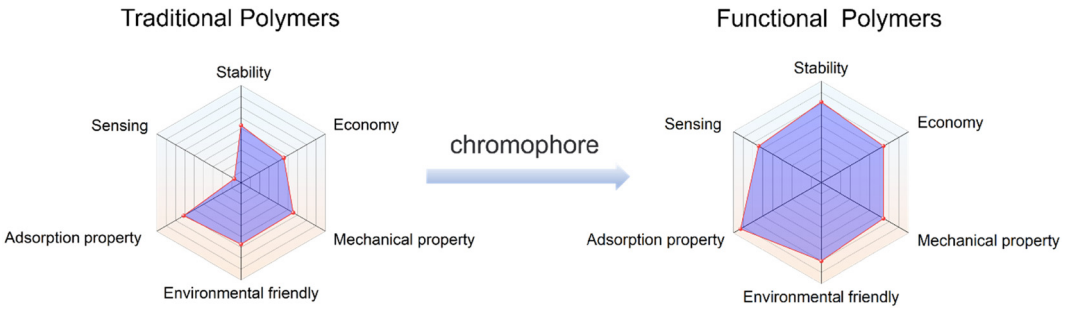

Fig. 10 A comparison of the strengths and weaknesses of the traditional polymers and functional polymers.

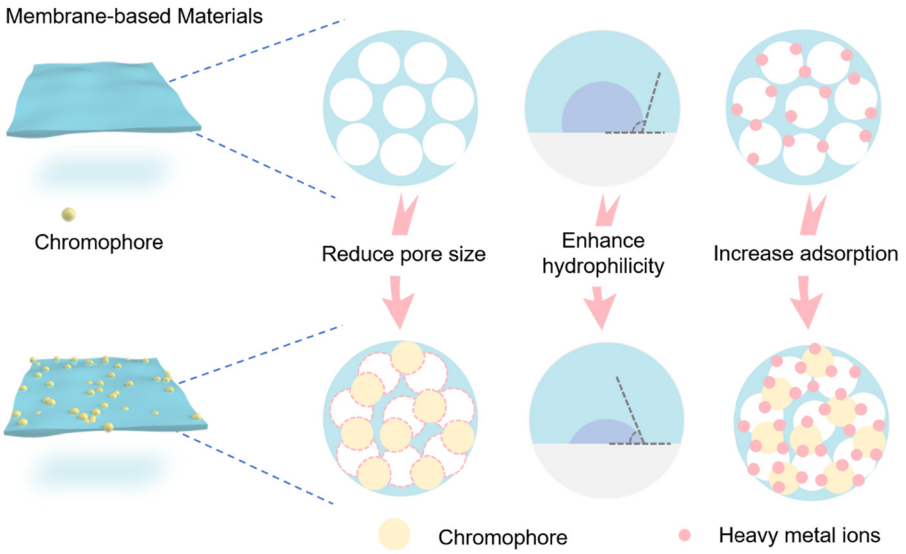

Fig. 11 Schematic diagram of preparation of functional membrane-based materials.

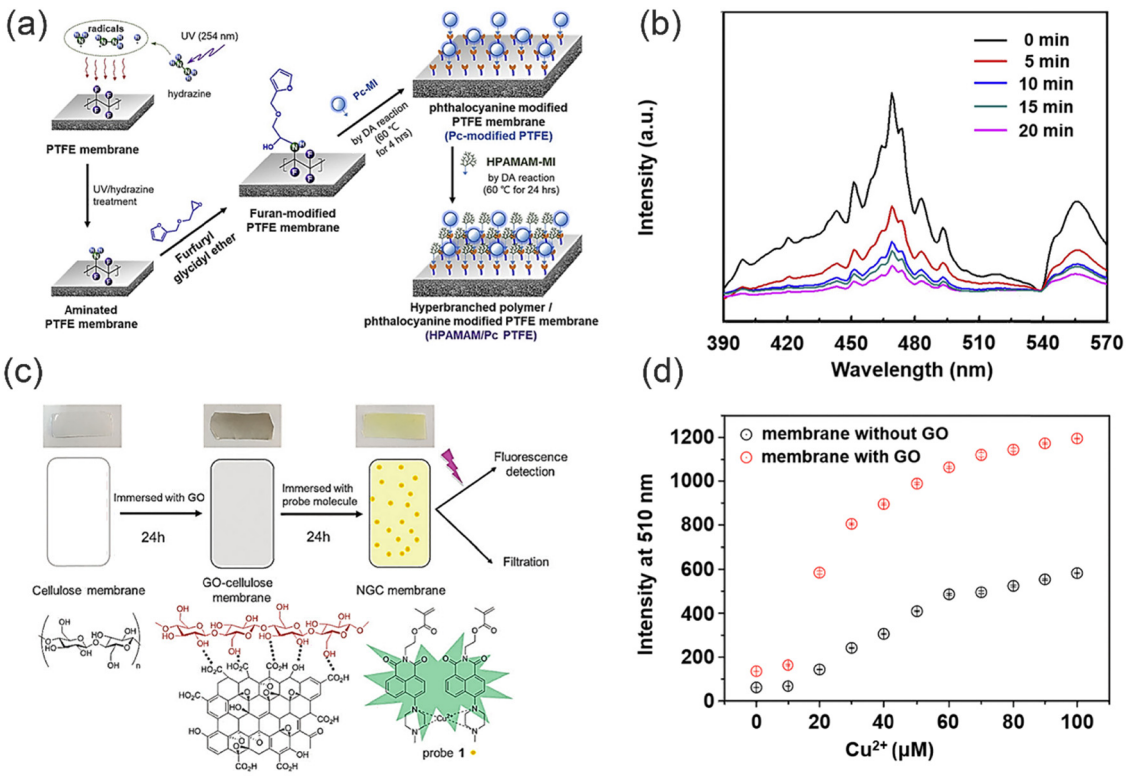

Fig. 12 The preparation of functional polymer membranes and their sensing and removal for heavy metal ions. (a) The preparation of HPAMAM/Pc PTFE membrane. (b) The fluorescence spectra of HPAMAM/Pc PTFE membrane with Cr(VI) ions adsorbed. Reproduced from ref. 97 with permission from Elsevier Ltd. Copyright 2019. (c) The comparison of the cellulose membrane, GO-cellulose membrane and modified NGC membrane. (d) Fluorescence intensity of probe 1 attached to the cellulose membrane with and without a GO coating.

permeation.[103–105] Moreover, the reversible Diels–Alder (DA) reaction between furan and maleimide moieties, operating under thermal conditions, endows the membrane with selective regenerative properties. Hence, the integration of multiple functional materials within a single membrane holds immense potential for enabling synergistic effects for a diverse range of applications. However, this functional membrane material faces the difficulties of complicated preparation and does not readily biodegrade. In general, using natural substances (*e.g.* cellulose, chitosan and lignin *etc.*) to synthesize polymers can fully reduce

the secondary pollution caused by the polymer adsorbents to the environment. Li and co-workers devised a biodegradable fluorescent cellulose membrane by direct dip-coating of graphene oxide (GO) with a naphthalimide fluorescence probe (Fig. 12c).[106] GO can be immobilized directly onto a cellulose surface *via* hydrogen bonding. The resulting composite material exhibits a significantly enhanced surface area, as confirmed by the Brunauer–Emmett–Teller (BET) measurement, which reveals an increase from 4.813 $m^2\ g^{-1}$ to 12.660 $m^2\ g^{-1}$. This marked increase in surface area provides a larger reaction interface, thereby facilitating a 300% increase in available binding sites for efficient removal of Cu^{2+}. Meanwhile, when Cu^{2+} coordinates with the nitrogen on the naphthalimide the fluorescence of the probe molecule changes (Fig. 12d). The detection limit and removal limit for Cu^{2+} were 7.3×10^{-7} M and 100 ppm. Notably, immersion of a cellulose film in the GO suspension engenders not only enhanced binding between the cellulose film and fluorescent molecules through augmented stacking, but also modulates the surface wettability. Following GO modification of the cellulose membrane, the contact angle between water drops and the film was observed to decrease from $81.0 \pm 0.31^\circ$ to $54.2 \pm 0.21^\circ$, reflecting a heightened hydrophilicity. EDS-mapping revealed that Cu^{2+} ions were uniformly distributed within the cellulose layer subsequent to filtration, indicating that Cu^{2+} removal was achieved *via* absorption. Furthermore, the even dispersion of Cu^{2+} throughout the membrane further suggests an effective adsorption process. In addition, the recyclability of the membrane materials indicates that the GO membranes exhibit good Cu^{2+} removal capacity even after several recycling cycles. This study presents a rapid and cost-effective methodology for fabricating fluorescent cellulose materials through doping with fluorophores. The resulting materials can be utilized for both heavy metal ion removal and sensing applications, which represents a convenient and versatile solution.

Dong and co-workers have successfully fabricated self-supporting flexible nanofiber membranes (NMs) composed of amidated polyacrylonitrile (aPAN) and branched polyethyleneimine (BPEI) *via* a facile electrospinning technique combined with a subsequent hydrothermal process (Fig. 13a),[107] in which NMs not only serve as strips for visual detection of Cu^{2+}, but also demonstrate excellent performance as adsorbents for the efficient removal of Cu^{2+} from water. The Cu^{2+} ions are captured by the aPAN/BPEI NMs, where they interact with the abundant amino groups in polyethyleneimine, resulting in a noticeable colour change in the NMs. This unique property allows for simultaneous detection and removal of Cu^{2+} with an impressive

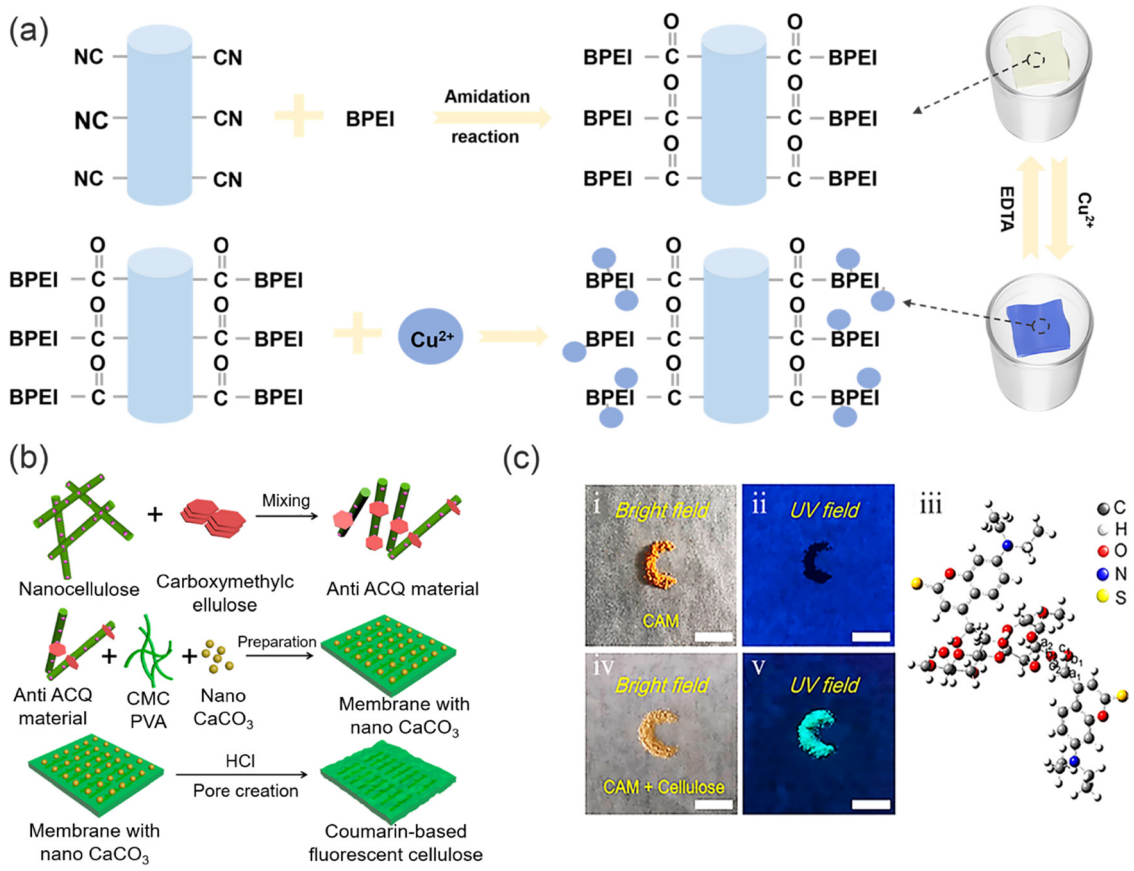

Fig. 13 The sensing and removal mechanism of functional polymer membranes for heavy metal ions in. (a) The preparation of aPAN/BPEI NMs and detection/removal of Cu^{2+}. Reproduced from ref. 107 with permission from American Chemical Society. Copyright 2021. (b) The preparation of anti-ACQ materials. (c) The optical image of CAM under natural light and ultraviolet light and the optical image of anti-ACQ material under natural light and ultraviolet light.

filtration capacity of 209.53 mg g^{-1}. The filtration process also facilitates preconcentration of Cu^{2+}, thereby further enhancing the sensitivity and adsorption capacity of the aPAN/BPEI NMs. Notably, the aPAN/BPEI NMs exhibit exceptional selectivity and recovery, accompanied by a simple treatment process. Furthermore, in contrast to powdered materials, the flexible and bulk self-supporting membranous structure of aPAN/BPEI NMs offers a significantly enlarged specific surface area, which facilitates the detection and absorption of Cu^{2+}, and allows for easy separation from aqueous solution, thereby greatly enhancing the operability of the materials and minimizing the risk of secondary environmental pollution. Nevertheless, further improvement in the sensitivity of aPAN/BPEI NMs is required. In 2019, Li and co-workers developed a new "cellulose spacer" strategy.[108] Specifically, when modifying the membrane with fluorescent dyes, conventional fluorophores are prone to experiencing aggregation-caused quenching (ACQ), which can potentially undermine their effectiveness in sensing applications. However, fluorescent solid nanomaterials can be prepared by assembling nanocellulose with coumarin based probe molecules (Fig. 13b and c). Nanocellulose exhibits hydrogen bonding interactions with hydroxyl-containing coumarin, which serves as a spacer that prevents the π–π stacking of coumarin. The membrane exhibits excellent sensing and filtration performance for Hg^{2+}, along with excellent recovery and biocompatibility. Therefore, the utilization of the "cellulose spacer" strategy for the assembly of fluorescent materials with sensing and removal capabilities holds great promise in various applications, particularly in the field of heavy metal ion sensing and removal. This approach offers a versatile and effective means to create fluorescent materials that possess desired properties, allowing for precise control over their performance. Such an approach spans a wide range of applications, making it a compelling method for addressing challenges in water treatment and heavy metal ion sensing.

The above composite membrane materials used for the effective detection and removal of heavy metal ions can be obtained by modifying simple membrane materials with fluorescent dyes and other small molecules. However, the ability of the membrane for the removal of heavy metal ions needs to be improved when compared with other polymeric materials.

3.2. Hydrogel-based materials

The distinct physical and chemical properties of hydrogels, including their intricate three-dimensional porous structure, abundant functional groups, binding sites, inherent hydrophilicity, exceptional swelling capacity, and facile modification, have sparked significant attention towards the advancement and utilization of novel hydrogel materials for the treatment of wastewater. Hydrogels have demonstrated remarkable efficacy in the adsorptive elimination of diverse inorganic pollutants, including heavy metal ions, as well as organic pollutants, such as toxic dyes.[109] Nevertheless, hydrogels crosslinked through physical means using natural polysaccharides such as chitosan or cellulose suffer from insufficient mechanical strength, instability in acidic environments, and limited active site diversity, thereby constraining their potential as versatile adsorbents.[110]

Significantly, the mechanical strength of a hydrogel can be improved by doping with nanomaterials (CDs, Fe_3O_4), and in addition additional functional groups from the CDs nanomaterials can provide additional binding sites for the adsorption of heavy metal ions. Notably, the three-dimensional mesh structure of the hydrogel can immobilize CDs, which makes them recoverable and as such they will not cause secondary contamination to the system during the detection and removal of heavy metal ions. Therefore, making the system cost-effective for the simultaneous detection and adsorption of heavy metal ions.[111,112] As such, the application of functionalized-hydrogels in the detection and removal of heavy metal ions has attracted much recent attention. For example, Wei and co-workers reported a novel carbon dot (CD-Fla) based system for the detection of toxic Pb^{2+} metal ions using a one-pot hydrothermal method using Ginkgo biloba flavonoid extracts as the raw material (Fig. 14a).[113] CD-Fla could be doped into an agarose hydrogel using H-bonding and dipole–dipole interactions. The as-prepared CD-Fla-doped hydrogel facilitated the simultaneous visual fluorescence detection and removal of Pb^{2+} from water. The prepared CD-Fla exhibited excellent biocompatibility and strong blue light emission and was selectively quenched by Pb^{2+} (Fig. 14b) enabling the quantitative detection of Pb^{2+} over a range from 0.1–20.0 nM. Meanwhile, the XPS and FTIR spectra indicted that the surface of the CD-Fla was rich in hydroxyl groups, which provided more adsorption sites for the removal of Pb^{2+}. The maximum adsorption capacity was determined to be 0.35 mg Pb^{2+} per milligram of CD-Fla. Notably, the fluorescent hydrogel could be regenerated using HCl solution after treatment the hydrogel could be re-used multiple times. Similarly, Wu and co-workers have developed a novel fluorescent nanocellulose hydrogel using the high ratio of cellulose nanofilaments (CNF) and high-performance luminescence of CDs, which serves as an effective adsorbent for heavy metal ion removal and an optical sensor for heavy metal ion detection (Fig. 14c).[114] The modification of CNF with CDs not only facilitates the hydroxyl-induced aggregation of heavy metal ions, enhancing the adsorption capacity, but also enables rapid visual response to heavy metal ions improving the stability of the fluorescence signal and sensitivity for determining heavy metal ions concentrations.[115,116] The CDs that are enveloped within intricate three-dimensional network structures have been employed as the fluorescent source for facilitating prompt visual detection of heavy metal ions. Subsequent to the adsorption and entrapment of heavy metal ions within the distinct structure of the synthesized fluorescent hydrogel, the fluorescence quenching effect of the heavy metal ions is enabled. Moreover, the three-dimensional network structure of the hydrogel promotes accelerated diffusion and aggregation of the heavy metal ions, facilitated by the high density of amide, hydroxyl, and carboxyl groups, thereby allowing efficient accumulation and adsorption of heavy metal ions. These properties highlight the potential of the developed fluorescent nanocellulose hydrogels as a promising platform for the sensitive and rapid detection of heavy metal ions in environmental and analytical applications. Remarkably, the maximum adsorption capacities of the

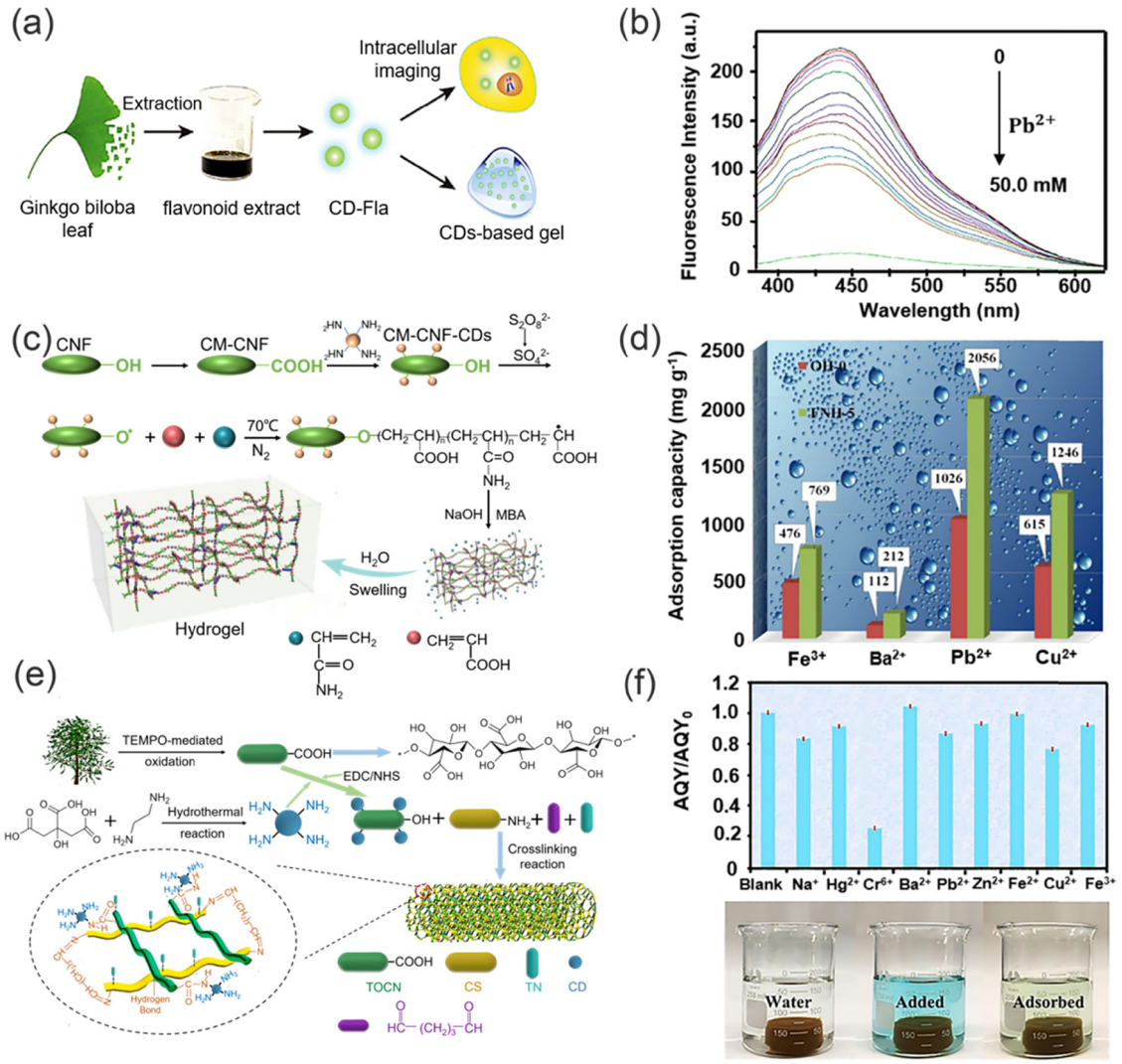

Fig. 14 The synthesis of green functional hydrogel polymers and their sensing and removal abilities for heavy metal ions. (a) The synthesis of CD-Fla hydrogel and its applications. (b) Fluorescence spectra of CD-Fla under different concentrations of Pb^{2+}. Reproduced from ref. 113 with permission from Springer Nature. Copyright 2018. (c) Fabrication of the fluorescent nano-cellulosic hydrogel. (d) The comparison of adsorption of heavy metal ions by synthetic hydrogel and original hydrogel. Reproduced from ref. 114 with permission from Royal Society of Chemistry Copyright 2019. (e) Synthesis of chitosan-based hydrogel. (f) Variations in absolute quantum yield (AQY) of the chitosan-based hydrogel in presence of different heavy metal ions. Reproduced from ref. 117 with permission from Elsevier B.V. Copyright 2021.

fluorescent hydrogels for Fe^{3+}, Ba^{2+}, Pb^{2+}, and Cu^{2+} were determined to be 769, 212, 2056, and 1246 mg g^{-1}, respectively (Fig. 14d). This innovative approach, combining the unique properties of CNF and CDs, results in a multifunctional nanocellulose hydrogel with enhanced performance for heavy metal ion removal and detection, offering novel insights into the design and fabrication of advanced materials for addressing pressing environmental challenges. Meanwhile, in 2020, a novel fluorescent chitosan-based hydrogel incorporating titanate and cellulose nanofibers modified with carbon dots was successfully synthesized for the efficient detection and removal of Cr(VI) (Fig. 14e).[117] Compared with the normal chitosan hydrogel without carbon dots, the fluorescent chitosan-based hydrogel exhibited sensitive detection and enhanced adsorption capacity for Cr(VI) (detection limit of 8.5 mg L^{-1} and maximum adsorption capacity of 228.2 mg g^{-1}), owing to the abundant amino and hydroxyl groups of the CDs and the high surface area of titanate providing additional binding sites for the removal of heavy metal ions. Moreover, the mechanical properties of the fluorescent chitosan-based hydrogels were enhanced after doping with titanate and CDs. The crosslinking reaction of chitosan and glutaric dialdehyde occurs to form a novel chitosan-based hydrogel in the presence of CDs and titanate nanofibers which were connected to the chitosan network by hydrogen bonding. The resulting hydrogel exhibited an interconnected network structure, facilitated by hydrogen bonding between the chitosan chains and the nanofibers. Notably, the amino groups on the chitosan chains facilitated the adsorption of Cr(VI) ions onto the surface of the hydrogel through electrostatic interactions. Moreover, the hydrogel exhibited a porous structure that served as an efficient mass transfer

channel, enabling rapid movement of Cr(VI) ions from the surface to the interior of the hydrogel. This unique characteristic was attributed to the porous nature of the fluorescent chitosan-based hydrogel, which enabled efficient internalization of the adsorbed Cr(VI) ions. Additionally, the CDs contained within the porous structures of the fluorescent chitosan-based hydrogel served as optical sensors for Cr(VI). Cr(VI) ions that were rapidly adsorbed on to the CDs due to electrostatic interactions, which resulted in fluorescence quenching. The fluorescent chitosan-based hydrogel exhibited a visual response for the highly efficient detection of Cr(VI) (Fig. 14f). The synthesis of this chitosan-based hydrogel with its unique structure, including the presence of CDs, titanate nanofibers, and a porous structure, represents a promising avenue for potential applications in areas such as environmental remediation and controlled release systems, owing to its efficient adsorption and mass transfer properties. These findings highlight the potential of these fluorescent chitosan-based hydrogels as promising materials for various practical applications and generating a significant contribution to the field of materials science and environmental chemistry.

Compared to single-signal fluorescence sensing, ratiometric sensing is more accurate and sensitive. In 2021, Li and co-workers designed a novel cellulose-based ratiometric fluorescent hydrogel (CDs-Rho). The ratiometric fluorescent probe was prepared using an amidation reaction between CDs as energy donor and rhodamine (Rho) as energy acceptor, and then the probe was loaded into a hydrogel to prepare a ratiometric fluorescent hydrogel.[111] CDs-Rho acts as a fluorescent unit, and the amino groups on the surface chelate with Hg^{2+}, leading to fluorescence quenching. Meanwhile, the carboxyl-rich CDs-Rho provides sites for Hg^{2+} chelation. In addition, the incorporation of CDs-Rho can effectively enhance the mechanical strength and improve the elasticity of the hydrogel. This fluorescent hydrogel was able to efficiently detect and remove Hg^{2+} from contaminated water. The probe exhibited a sensitive linear response to Hg^{2+} over a range from 0–100 μM, with a lower limit of detection of 2.19×10^{-9} M and exhibited higher selectivity towards Hg^{2+} than other cations. In addition, the fluorescent hydrogel displayed a removal efficiency of ~95% for Hg^{2+}, which was higher than for traditional hydrogel materials. Importantly, the fluorescent hydrogel maintained a high adsorption efficiency after five consecutive cycles of use and does not cause secondary contamination. Therefore, this system provides a promising strategy for the effective identification and removal of heavy metal ions. Most fluorescent hydrogels are formed by first preparing the CDs and then integrating them into the hydrogel to form a fluorescent hydrogel that can simultaneously detect and adsorb heavy metal ions (Fig. 15a). However, fluorescent hydrogels obtained through non-covalent binding face problems such as low loading efficiency and poor stability in complex environments. To overcome the challenge of low loading efficiency in functional materials prepared by immersion, which leads to reduced sensitivity and stability. Wu and co-workers employed cellulose nanofibers as the raw material and employed a one-pot hydrothermal method for the single-step fabrication of fluorescent hydrogels with *in situ* formation of carbon dots (Fig. 15b).[118] The resultant functional material exhibited remarkable capability for the detection and removal of Hg^{2+}. The fluorescent hydrogel synthesized *via* this approach not only exhibited good mechanical strength, but also exhibited outstanding fluorescence properties and adsorption capacity. By integrating the synthesis of probes and substrates within a unified process, the one-pot hydrothermal method both circumvented the need for separate preparation steps and significantly enhanced the detection sensitivity and stability of the functional materials. This expedient and efficient synthetic strategy offers significant promise for advancing the development of sustainable sensing and detection materials

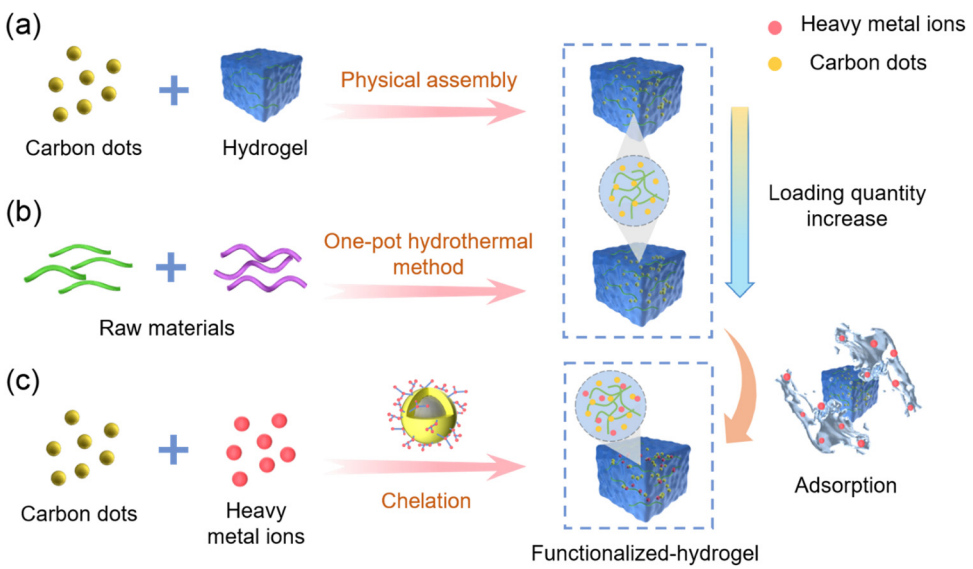

Fig. 15 The preparation of functional hydrogels using different methods. (a) Impregnation method. (b) One-pot hydrothermal process. (c) Interaction between fluorescent probes and heavy metal ions.

and systems. Similarly, Zhang and co-workers directly employed nitrogen-doped carbon dots (N-CDs) synthesized by low-temperature sintering to form hydrogels upon coordination with heavy metal ions (Fig. 15c).[119] Specifically, due to the abundant –COO–, –CO–, NH–, –NH–, and –OH groups on N-CDs, negatively charged N-CDs bind to various positively charged heavy metal ions (Pb^{2+}, Cu^{2+}, Ni^{2+}, Co^{2+}, Cd^{2+}) in water through electrostatic interaction and coordination, forming hydrogels and removing heavy metal ions from water. Fluorescence and UV spectroscopy analyses show that N-CDs can sensitively detect Pb^{2+} in water, with a detection limit of 3 ppb. The rapidly formed hydrogel can effectively remove a variety of heavy metal ions and can be easily separated from treated wastewater over multiple cycles. The simple and creative method of using a hydrogel formation process to remove heavy metal ions directly is particularly attractive and worthy of additional investigation.

Although fluorescent hydrogels exhibit excellent capabilities in the detection and removal of heavy metal ions. The metal ions take a long time to diffuse to the adsorption sites, which limits further application of this type of fluorescent hydrogels.

3.3. Aerogel-based materials

Aerogels represent a class of nanostructured, low-density bulk materials with rigid skeletal frameworks, porous structures and open pores, which can be meticulously tuned at the nanoscale. These unique characteristics provide aerogels exceptional physical properties, including ultra-high specific surface areas and unprecedented adsorption capacities. As a result, aerogels have emerged as highly promising materials for a wide spectrum of applications, including sensors,[120] chemical adsorption,[121] catalyst supports,[122] biomedical devices,[123] thereby propelling advancements in the field of environmental protection. In addition, by modifying aerogels with nanomaterials (CDs, AuNPs and Fe_3O_4), aerogels can attain even more properties, for example, aerogels doped with CDs can gain the ability to detect and adsorb heavy metal ions simultaneously, and can exhibit enhanced mechanical stability compared with pure aerogels, as well as displaying greater efficiency for heavy metal ion removal. Meanwhile, the three-dimensional skeleton of an aerogel can immobilize CDs, which improves their fluorescence stability and reusability, which enhances the efficiency and environmental friendliness of CDs for heavy metal ion detection.

Wang and co-workers reported a novel porous MoS_2-based composite aerogel (Fig. 16a).[124] Specifically, the composite

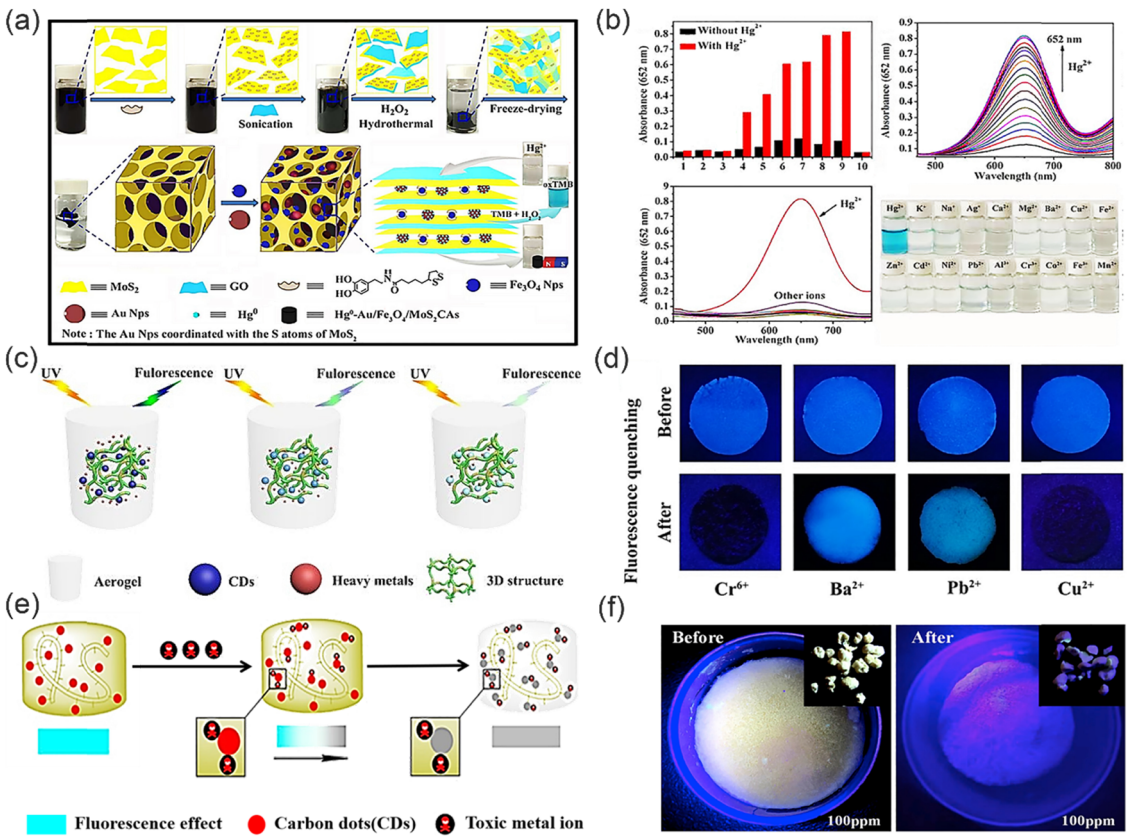

Fig. 16 Synthesis of functional fluorescent aerogels and their mechanism of sensing and removing heavy metal ions. (a) The detection mechanism of Au/Fe_3O_4/MoS_2CAs for Hg^{2+}. (b) The fluorescence spectra and adsorption properties of Au/Fe_3O_4/MoS_2C for Hg^{2+}. Reproduced from ref. 124 with permission from American Chemical Society. Copyright 2016. (c) The mechanism of the adsorption and fluorescence sensing of Cr(VI). (d) The fluorescence quenching image in presence of different heavy metal ions. Reproduced from ref. 125 with permission from Royal Society of Chemistry. Copyright 2020. (e) The mechanism of detection and removal of heavy metal ions by CQDs/NFC composite aerogel. (f) The optical image of fluorescent aerogel under ultraviolet light before and after adsorption. Reproduced from ref. 126 with permission from Elsevier B.V. Copyright 2020.

aerogel was prepared from graphene oxide (GO) and molybdenum disulfide flakes, and then gold and iron tetroxide nanoparticles (NPs) were embedded within the GO-doped molybdenum disulfide flakes, respectively, thereby obtaining porous Au/Fe_3O_4/MoS_2CAs aerogels. In this system, the AuNPs as a fluorescence source can specifically bind to Hg^{2+} to form a gold amalgam, thus detecting and removing Hg^{2+} (Fig. 16b). Meanwhile, the aerogel has a porous structure and thus enhanced binding sites, which can provide sufficient binding sites for Hg^{2+}. Moreover, the morphology and pore size of the aerogel can be adjusted by changing the doping amount of GO, which can effectively improve the mechanical properties of the aerogel. The detection limit of the functional aerogel for Hg^{2+} was 3.279 nM, and the adsorption capacity is about 1527 mg g^{-1}. Such a low detection limit and high adsorption capacity make the functional aerogel outstanding amongst similar materials. In addition, because of the magnetic properties of the Fe_3O_4 nanoparticles, the composite aerogels were easily magnetically separated after doping with Fe_3O_4, which is beneficial for the recovery and multiple repeated uses of the aerogels. Significantly, the Au/Fe_3O_4/MoS_2CAs aerogels still exhibited high removal efficiency (>95%) after 10 times of continuous recycling. However, although the composite aerogel has excellent heavy metal ions detection and removal capabilities, the preparation process is costly and requires the introduction of additional metal ions (from the aerogel), which may cause secondary contamination. Therefore, the development of aerogels that are cheap and easily available and environmentally friendly are in demand. In 2020, Wu and co-workers developed and prepared a novel fluorescent aerogel with a three-dimensional meshwork structure (Fig. 16c) using highly photoluminescent CDs and renewable natural carboxymethylated cellulose nanofilaments (CM-CNF).[125] Fluorescent carbon dots were obtained by hydrothermal reaction, and then the fluorescent carbon dots were soaked and integrated into the CM-CNF aerogel by hydrogen bonding to obtain a composite aerogel for the simultaneous detection and removal of Cr(VI) (CDs-CM-CNF). The fluorescent CDs encapsulated within the novel aerogel network structures exhibit abundant amino, carboxyl, and hydroxyl groups. This unique composition enables these CDs to serve as a highly sensitive and rapid visual source for the detection of Cr(VI) ions, as demonstrated in Fig. 16d. Furthermore, the abundance of adsorption sites on the aerogel surface facilitates the rapid aggregation of Cr(VI) ions, driven by electrostatic interactions with the positively charged amino groups. This phenomenon promotes the diffusion of anionic $Cr_2O_7^{2-}$ ions to the surface of the synthesized aerogel, effectively enhancing the efficiency for Cr(VI) adsorption. The maximum adsorption amount reached was 433.5 mg g^{-1}. This architecture and composition of the aerogel-encapsulated CDs offer a promising approach for the efficient detection and removal of Cr(VI) ions, with potential implications in environmental and analytical applications. Similarly, Guo and co-workers developed a novel carbon quantum dot (CQDs)/nanocellulose (NFC) composite aerogel prepared using a green chemical synthetic method and applied it for the adsorption and detection of heavy metal ions (Cr^{3+}) in water (Fig. 16e).[126] CQDs and NFCs are directly bonded to each other by intermolecular forces or hydrogen bonds, without the addition of additional cross-linking agents which is adventitious since those reagents could result in contamination. The composite aerogel formed this way does not change the original structure of CQDs and NFCs. However, in the presence of Cr^{3+}, CQD exhibits excellent fluorescence response (Fig. 16f). In addition, the presence of abundant amino and hydroxyl groups on the surface of the CQDs provides additional adsorption sites for the removal of Cr^{3+}, which enhances the removal efficiency of the composite aerogel. The three-dimensional structure of the NFC aerogel provided a good carrier for CQDs, which made it possible to repeat the detection and removal of Cr^{3+} repeatedly. The synergistic effect of the CQDs and aerogel enhanced the detection and removal efficiency for heavy metal ions, and in addition the composite aerogel does not undergo toxic chemical reactions or produce toxic substances during the whole process of adsorption of Cr^{3+} pollutants in water, which enhances the environmental friendliness of this composite material. This study provides a new method for the preparation of green adsorbents with the synergistic effect of adsorption and fluorescence. In 2022, Han and co-workers successfully fabricated multifunctional aerogels by employing waste collagen, polyethyleneimine (PEI), and carbon dots, which are cross-linked with aldehyde cellulose nanofibers, for the purpose of detecting and adsorbing Cr(VI) ions. This approach demonstrates the utilization of sustainable materials and advanced nanotechnology for environmental applications (Fig. 17a).[127] With this system, CDs are attached to the aerogel network by hydrogen bonding. Upon immersion of the aerogel in a solution containing Cr(VI) ions, rapid adsorption of the ions onto the surface of the aerogel, enriched with numerous amino groups, occurs due to strong electrostatic interactions with the positively charged amino groups on surface of CDs (Fig. 17b). The resulting aerogel skeleton, featuring a three-dimensional network structure, serves as an efficacious adsorbent and trapping agent for heavy metal ions.[128] Notably, fixing the CDs with high quantum yield within the 3D framework enhances the stability of the fluorescence signal.[125] While the synergistic effects of the CDs and aerogel enhances the removal efficiency for Cr(VI). Stress–strain curves indicated that the aerogel containing CDs exhibited good mechanical strength compared with the aerogel without CDs. In addition, the aerogel loaded with CDs could be recycled several times and maintained good removal efficiency. The resulting aerogels exhibit exceptional performance in terms of both detection sensitivity and adsorption capacity, making them promising candidates for efficient and sustainable remediation of Cr(VI) contamination.

However, most composite aerogels used for detection and removal of heavy metal ions are simply discarded after multiple uses, which may cause damage to the environment. How to dispose of the used composite aerogels is a problem that needs to be solved. Towards solving this important problem, Li and co-workers fabricated porous fluorescent aerogels, denoted as CPC aerogels, through the immersion of amino-functionalized carbon dots (CDs-NH_2) into a three-dimensional network of PEI and carboxymethylated cellulose (CMC) aerogels. This aerogel

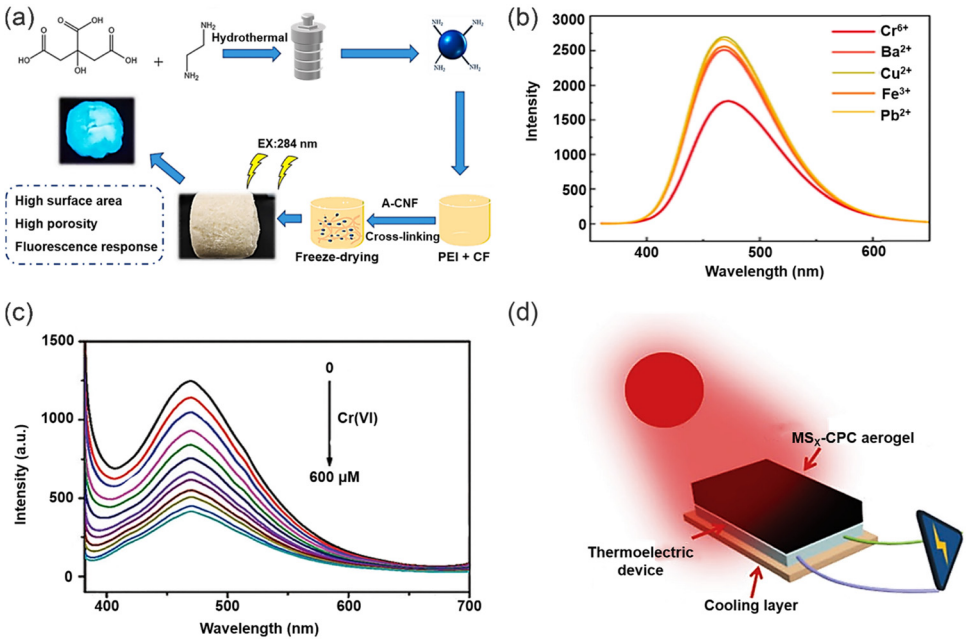

Fig. 17 The sensing and removal of functional aerogels for heavy metal ions and their resource utilization. (a) The synthesis of fluorescent aerogel. (b) Fluorescence spectra of fluorescent aerogel in presence of different heavy metal ions. Reproduced from ref. 127 with permission from Elsevier B.V. Copyright 2022. (c) Fluorescence spectra of the CPC aerogel under different concentrations of Cr(VI). (d) Schematic diagram of a rotating motor driven using the solar-powered thermoelectric generator.

allowed for simultaneous detection and adsorption of Cr(VI) ions.[129] The CPC aerogels exhibited a linear response to Cr(VI) over a concentration range from 0–600 $\times$ 10^{-6} M (Fig. 17c). Moreover, the aerogel can effectively remove Cr(VI) ions by electrostatic and chelating effects, with a maximum adsorption capacity of 354.61 mg g^{-1} for Cr(VI). Remarkably, following the adsorption of Cr(VI), the CPC aerogel can be vulcanized (MSx-CPC gel), resulting in the formation of MSx-CPC gel, which can be utilized for solar thermoelectric power generation to generate electricity (Fig. 17d). In addition, the MSx-CPC gel demonstrates a remarkable evaporation rate of approximately 1.31 kg m^{-2} h^{-1} under one sun solar irradiation, making it an ideal candidate for solar steam generation. This approach provides new uses for aerogels after adsorption of heavy metal ions. Therefore, providing a new paradigm for researchers working towards multiple use aerogels that can be up-cycled.

3.4. Other polymer materials

In addition to, hydrogel and aerogel polymers, other polymer-based materials have been developed to detect and remove heavy metal ions in various environments. For example, in 2017, Liu and co-workers developed a simple one-pot method for the synthesis of luminescent AuNPs with sponge-like networks (Fig. 18a).[130] The luminescent AuNPs could be prepared using pentaerythritol tetrakis 3-mercaptopropionate (PTMP) as both reducing and surface coating ligand. The specific and strong D^{10}–D^{10} interactions between AuNPs and Hg^{2+} resulted in sensitive and selectivity sensing of Hg^{2+} (Fig. 18b). The use of PTMP as a cross-linker in the formation of the three-dimensional sponge-like network of AuNPs not only promotes the structural integrity of the network, but also enhances the luminescent properties of the AuNPs. This innovative one-pot synthesis strategy circumvents the challenges associated with the incompatibility between the formation of sponge-like structures and the stability of AuNPs luminescence, which are commonly encountered in conventional methods. Furthermore, the unique combination of the highly porous sponge-like structure and the strong metallophilic Hg^{2+}–Au^{+} interactions result in a remarkable saturation capacity of 2.48 g Hg^{2+} per gram of sorbent for the novel AuNPs-based sponge-like network, surpassing the capacities reported for typical mercury absorbents. This approach represents a significant advancement in the fabrication of highly efficient and stable mercury sorbents with potential implications in environmental remediation and pollution control. Yan and co-workers devised and fabricated a novel chitosan–gold nanocomposite, which has been integrated into functionalized paper strips for the purpose of visual sensing and removal of trace amounts of Hg^{2+} ions (Fig. 18c).[131] Notably, this nanocomposite exhibits exceptional response towards Hg^{2+} ions in solution, as evidenced by the impressive detection limit of 3.2 $\times$ 10^{-9} M (Fig. 18d). This remarkable sensitivity is attributed to the reversible formation of gold amalgam between the gold nanoparticles and Hg^{2+} ions. Moreover, the gold nanochromophores were dispersed with minimal aggregation due to the chitosan and the filter paper, which effectively prevents the ACQ effect. Meanwhile, due to the multiple hydroxyl groups and free amino groups of the chitosan–gold nanocomplex, it was able to remove Hg^{2+} from solution. Furthermore, the fabrication process of chitosan–gold nanocomplexes is straightforward, making them suitable for

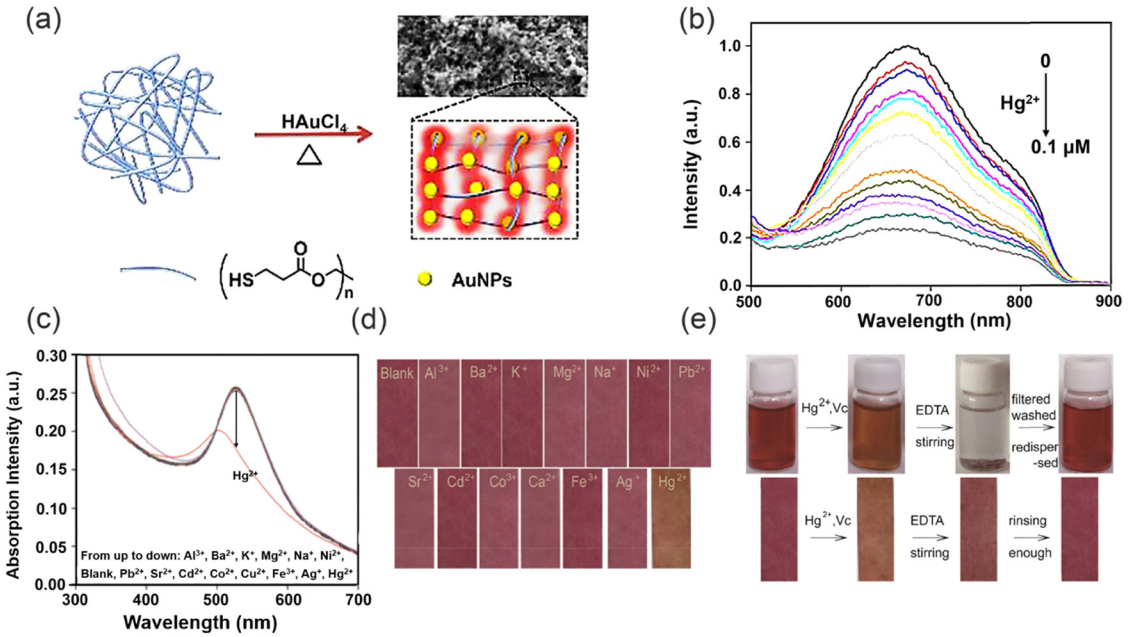

Fig. 18 Synthesis of metal-based nanopolymers and its detection-removal for heavy metal ions. (a) The synthesis of the luminescent sponge-like network of AuNPs. (b) The fluorescence spectra of PTMP-AuNPs under different concentrations of Hg^{2+}. Reproduced from ref. 130 with permission from Royal Society of Chemistry. Copyright 2017. (c) The selectivity of the proposed chitosan–AuNP system (d) the color change of chitosan–AuNP functionalized paper-strips. (e) The reversibility of chitosan–AuNP solution and its functionalized paper-strips. Reproduced from ref. 131 with permission from Royal Society of Chemistry. Copyright 2019.

repeated utilization in detecting trace amounts of Hg^{2+} in various environmental aqueous solutions as well as fruit or vegetable juice samples (Fig. 18e).

However, a crucial consideration in the utilization of metal nanoparticles for detecting heavy metal ions is the inevitable co-introduction of other metal ions. Additionally, the inherent limitations of high costs and low adsorption capacity pose significant challenges to the advancement of such metal nanomaterials. Addressing these issues is imperative for researchers working towards the treatment and recovery of heavy metal ions, and represents a crucial aspect that requires further improvement in order to enhance the efficacy of these materials.[132,133] Xu and co-workers designed an environment-friendly fluorescent sensing platform towards Au^{3+} detection and removal (Fig. 19a).[134] Versatile fluorescent microspheres, specifically melamine formaldehyde microspheres (MF), incorporating nitrogen and sulfur co-doped carbon dots (N,S-CDs), were synthesized *via* the MF pre-polymer incorporation process. The highly branched MF pre-polymer exhibited remarkable efficacy in efficiently integrating fluorophores under acidic catalysis and elevated heating conditions. Stable fluorescent microspheres (MF-CDs) can be obtained by doping the MF prepolymer with CDs. Fluorescence quenching of the N,S-CDs by Au^{3+} was observed (Fig. 19b), attributed to the non-radiative electron-transfer process from N,S-CDs to Au^{3+} ions, facilitated by the strong affinity between Au and the N/S species.[135] This remarkable fluorescence sensing ability of the MF-CDs stemmed from the synergistic effect of the amplification of the MF substrate and the collective contribution of N, and S-CDs towards the fluorescence response of the MF-CDs.[136–138] Specifically, in an acidic environment, Au^{3+} primarily exist as $AuCl_xOH_{(4-x)}^-$ in solution while the MF was protonated, promoting electrostatic interactions between Au^{3+} and the MF matrix,[139] in addition to the inherent affinity of gold for nitrogen.[140] As a result, Au^{3+} is captured and enriched on the surface of the MF *via* enhanced local concentration around the nitrogen and N,S-CDs immobilized on the MF-CDs. Furthermore, the high density of N,S-CDs on the MF-CDs provides abundant binding sites for Au^{3+}, facilitating the interaction of a single Au^{3+} ion with multiple N,S-CDs and promoting cooperative processes that strengthen fluorescence quenching. Additionally, the MF-CDs exhibit remarkable adsorption capacity for Au^{3+}, with an adsorption capacity of up to 1 mmol g^{-1} when used as an adsorbent. Notably, the adsorption of Au^{3+} onto the MF-CDs results in an *in situ* conversion to AuNPs, leading to the formation of an immobilized nanocatalyst, denoted as MF-CDs-AuNP. This nanocatalyst exhibits remarkable recyclability and efficiently reduces 4-nitrophenol, showcasing its potential for sustainable catalytic applications. In addition, the selectivity of the fluorescence response towards Au^{3+} indicates superior performance compared to other assessed metal ions. The fluorescent CDs exhibit exceptional sensitivity and rapid response for the detection in real samples, without the use of organic solvents or harmful dyes, which is highly advantageous for wastewater purification, and holds great promise for environmentally sustainable applications in water treatment. Similarly, in 2021, Chai and co-workers developed a novel dual-function Fe_3O_4–Carbon dots nanocomposite (Fe_3O_4/CDs) based magnetic fluorescent probe for the detection and recovery of Hg^{2+} through a hydrothermal method (Fig. 19c).[141] The Fe_3O_4/CDs exhibited numerous

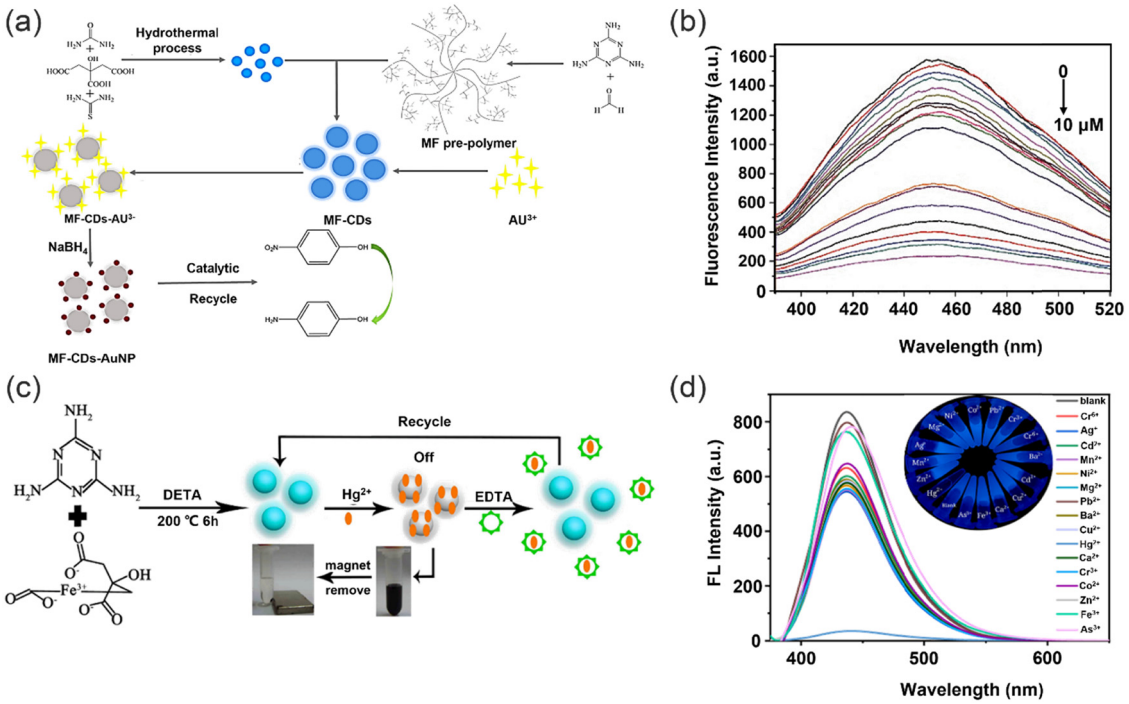

Fig. 19 Preparation of polymer sensors and their detection and removal of heavy metal ions. (a) The synthesis and applications of fluorescent microspheres. (b) The effect of pH on the detection of Au^{3+}. Reproduced from ref. 134 with permission from Elsevier B.V. Copyright 2021. (c) The synthesis Fe_3O_4/CDs and utility in sensing and removal of Hg^{2+}. (d) Fluorescence spectra of probe in presence of different heavy metal ions. Reproduced from ref. 141 with permission from Elsevier Ltd. Copyright 2021.

advantageous features compared to existing single-function probes, including remarkable Hg^{2+} removal capability, reusability, excellent environmental tolerance, and cost-effectiveness. With this sensing system, Hg^{2+} can efficiently coordinate onto the surface of Fe_3O_4/CDs by means of electrostatic interactions and quench the fluorescence signal of Fe_3O_4/CDs as a result of fluorescence charge transfer (turn-off) (Fig. 19d), with a limit of detection of 0.3 nM. Notably, the inherent magnetic properties of Fe_3O_4/CDs enabled the removal of Hg^{2+} from contaminated water, thus conferring significant advantages for environmental remediation applications. Moreover, the Fe_3O_4/CDs could be recycled by the addition of EDTA solution, highlighting their potential for real sample analysis, thus underscoring the practical utility of this composite material in addressing the pressing issue of Hg^{2+} contamination in natural bodies of water.

Moreover, supramolecular polymers containing DNA have been regarded as promising candidates for the selective sensing and efficient removal of heavy metal ions, thereby complementing the use of nanomaterial-based polymers. For example, in 2017, Wu and co-workers reported the construction of a supramolecular system generated by the self-assembly of thymine substituted copolymer aromatics and tetraphenylene (TPE) derivatives in the presence of Hg^{2+}.[142] The thymidine group of the copolymer tightly coordinates with Hg^{2+} *via* the T–Hg^{2+}–T pair. The interaction between the aromatics and the butyronitrile groups of the TPE derivatives forms a crisscrossed fluorescent network structure. In addition, AIE of the supramolecular polymers results in high fluorescence, facilitating the detection and removal of Hg^{2+} (Fig. 20a) with a limit of detection 2.3 μM, and stable fluorescence from Hg^{2+} in the presence of competing ions. Which is a testament to the exceptional selectivity of this supramolecular system towards Hg^{2+}. The fluorescence due to Hg^{2+} was still evident in the presence of other competing ions, confirming remarkable selectivity of this supramolecular system for Hg^{2+}. While the addition of Na_2S to the supramolecular polymer allows for recovery of the polymer for re-use. The removal efficiency for Hg^{2+} can reach more than 96%. Significantly, the system exhibits almost no loss of activity when recycled for the sensing and trapping of Hg^{2+}. In 2019, Yang and co-workers enhanced the properties of the supramolecular polymer, endowing it with rapid reaction rate and superior selectivity, whilst also achieving fast adsorption kinetics and high adsorption capacity towards the efficient removal of Hg^{2+}. A fluorescent supramolecular polymer featuring AIE was fabricated using supramolecular host–guest interactions, which involved a biphenyl-extended pillar arene decorated with two thymine sites as arms (H) and a tetraphenylethylene (TPE)-bridged bis (quaternary ammonium) guests (G).[143] Most notably, the method of combining AIE with a supramolecular strategy provides a suitable method for the selective detection (Fig. 20b) and rapid removal of Hg^{2+} and provides scope for the design of new adsorbent materials. Moreover, the strong bonding of the T–Hg^{2+}–T pair between the thymine group and Hg^{2+} makes the supramolecular polymer easily generate a supercross-linked network, which results in a multifunctional Hg^{2+} absorbent. The material can reach more than 90% Hg^{2+} removal efficiency, and the emission increases linearly with Hg^{2+} concentration over a range

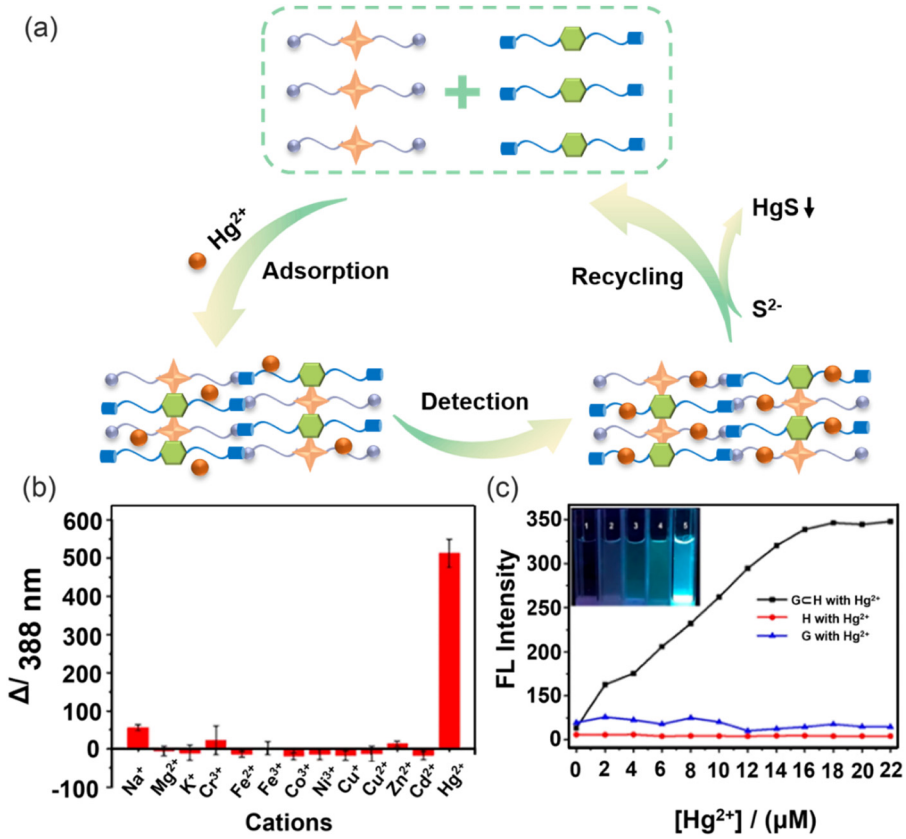

Fig. 20 Supramolecular host–guest interactions of biomaterials for the detection and removal of heavy metal ions. (a) Mechanism of polymers for the detection and removal of heavy metal ions. (b) Fluorescence emission of G⊂H with the addition of different metal ions in aqueous solutions. (c) Variation of fluorescence intensity of G⊂H with the increasing concentration of Hg^{2+}. Reproduced from ref. 143 with permission from American Chemical Society. Copyright 2019.

from 0–15 μM. When the concentration of Hg^{2+} was added gradually, the emission intensity of the supramolecular polymer dramatically increased and the fluorescence was significantly enhanced under UV light irradiation (Fig. 20c) with a detection limit of 3×10^{-7} M.

4. Luminescent porous materials

Porous materials are polymer materials with high specific surface area containing networks of interconnected pores. Based on the size of the pores, porous materials can be divided into three categories, which includes micropore materials (less than 2 nm), mesoporous materials (around 2–50 nm), and macropore materials (more than 50 nm),[144] which includes zeolites, metal organic frameworks (MOFs), covalent organic frameworks (COFs) and organic polymers.[145] Since polymers have been introduced above, they will not be covered in this section. Porous materials exhibit good scalability, long-term stability, selectivity and high adsorption capacity, but also exhibit excellent processability and low cost.[146,147] The advantages of porous materials make them suitable for the detection and adsorption of heavy metal ions in water. In the detection and adsorption process, the most significant advantage of COFs and MOFs as luminescent porous materials is that they provide the same interaction site with heavy metal ions, making their interaction with heavy metal ions more effective (Fig. 21).

4.1. COF-based materials

Covalent organic frameworks (COFs) are a type of crystalline porous material constructed using organic building blocks.[148,149] Because of their excellent chemical/thermal stability, porosity, and flexible topological connectivity, COFs are ideal materials with intrinsic "all-in-one" sensing functionalities for the detection and adsorption of heavy metal ions.[150] The controllable pores of COF materials can act as active sites, which are capable of accommodating guest molecules, including heavy metal ions.[151] Furthermore, the internal surface of the COF feature diverse functional groups, including amino, carboxyl, or hydroxyl groups,[152,153] enabling synergistic interaction with heavy metal ions to form strong coordination bonds. This facilitates the specific and selective binding of heavy metal ions, endowing COF materials with the capability to detect and adsorb heavy metal ions.

The synergistic effects of chelating groups in porous COFs helps with efficient detection and removal of heavy metal ions.

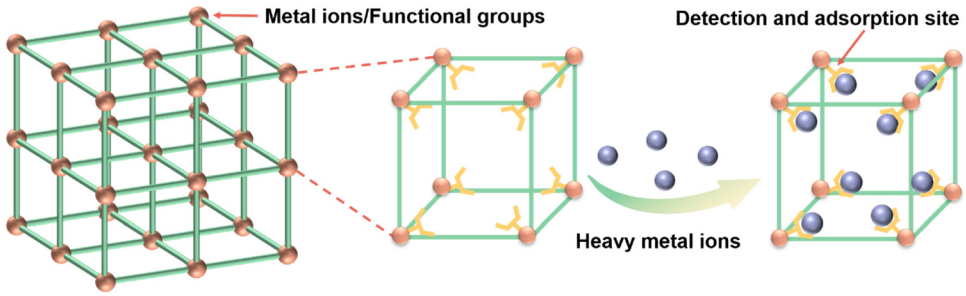

Fig. 21 Coordination interactions between MOF/COF frameworks and heavy metal ions.

The properties of COFs are improved by the rational placement of various functional groups in the COF framework. For example, Wang and co-workers designed a thioether-functionalized COF, COF-LZU8, for the selective detection and easy removal of Hg^{2+}.[154] Due to the porous structure of COFs, the thioether groups can be uniformly distributed in the pores and can interact with Hg^{2+} (Fig. 22a). The detection limit for Hg^{2+} was determined to be 25.0 ppb. The fluorescence spectra of COF-LZU8 in the solid state exhibits a maximum emission band at 460 nm and a quantum yield of 3.5% upon excitation at 390 nm. Since the structure of COFs can avoid the ACQ effect, COF-LZU8 exhibits high fluorescence (Fig. 22b). Moreover, the straight-through channel in the topology of COFs facilitates direct contact between S atoms and Hg^{2+}, thus facilitating efficient heavy metal ion removal. For solutions containing very low concentrations of mercury, COFs can achieve removal rates of over 98%. The stable hydrazone bond in the structure of COF-LZU8 makes it very stable in standard organic solvents and water, which also ensures the effective recovery of COF-LZU8. Yuan and co-workers designed an allyl and hydroxyl functionalized hydrazone-linked AH-COF, for the exclusive detection and effective removal of Hg^{2+}.[155] The ordered pore structure of COFs allows the allyl and hydroxyl groups to be uniformly distributed in the COFs framework. In addition, allyl and hydroxyl groups as the exclusive reaction receptor sites for Hg^{2+} also ensure the detection and removal of Hg^{2+}. Due to the extension of the π-conjugated structure in the AH-COF framework, AH-COF exhibits fluorescence (Fig. 22c) and the fluorescence spectra of AH-COF in acetonitrile solution can reach a fluorescence quantum yield of 3.8% at an excitation wavelength of 420 nm, compared with just 0.9% for the monomers and the

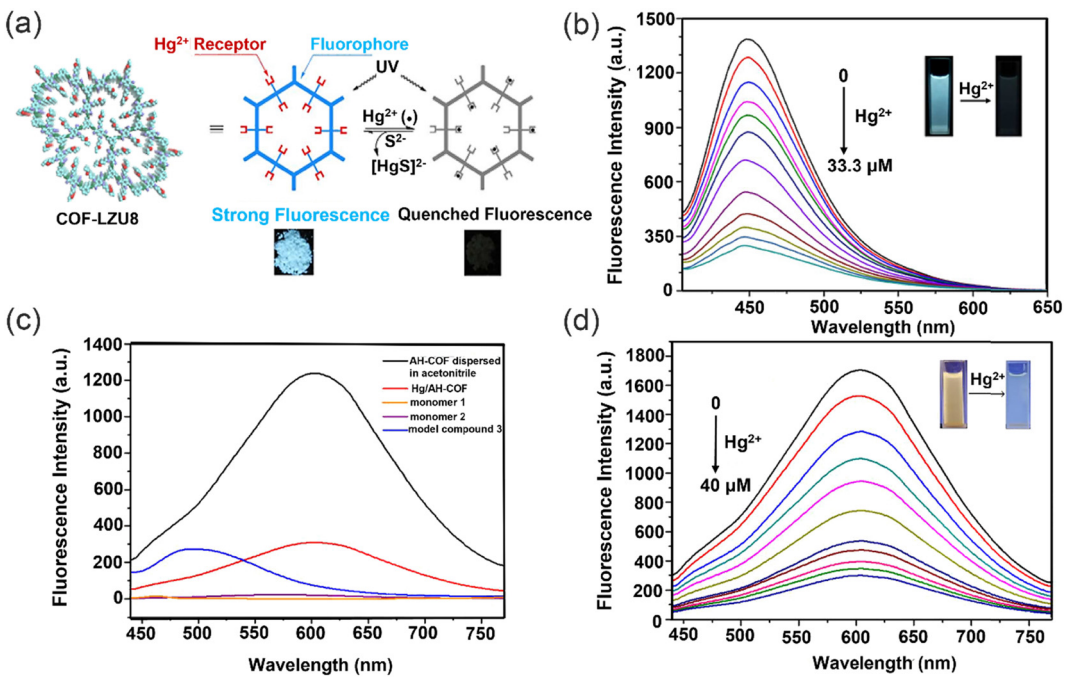

Fig. 22 Synergistic effect of chelating groups in porous COFs for the detection and removal of heavy metal ions. (a) The sensing and removing mechanism of COF-LZU8 for Hg^{2+}. (b) Fluorescence intensity of COF-LZU8 with the addition of Hg^{2+}. Reproduced from ref. 154 with permission from American Chemical Society. Copyright 2016. (c) Fluorescence spectra of AH-COF (black) and Hg/AH-COF (red). (d) Fluorescence intensity of AH-COF dispersed in acetonitrile with Hg^{2+}. Reproduced from ref. 155 with permission from Elsevier B.V. Copyright 2020.

corresponding model small-molecule compound. AH-COF was also selective and sensitive to Hg^{2+} in the presence of competing ions (Fig. 22d). Significantly, AH-COF can be easily recovered and recycled by adding $NaBH_4$.

Disappointingly, the sensitivity and fluorescence efficiency of COFs in the above examples are relatively low, which can hinder the exploration of COFs for fluorescence sensing. To address this issue, more flexible linkers can be incorporated. In 2019, Qiu and co-workers developed a COF named TFPPy-CHYD by combining 1,3,6,8-tetrakis(4-formylphenyl)-pyrene (TFPPy) with a carbohydrazide (CHYD) linker with highly luminescent properties and a quantum yield of 13.6%.[156] The detection limit for Hg^{2+} was 17 nM and the adsorption capacity for Hg^{2+} was 758 mg g^{-1} (Fig. 23a). The π–π stacking between COFs frameworks is affected by the CHYD-linked unit, which enhances the luminescence of TFPPy-CHYD. In addition, the homogeneous porous structure of the COFs allows the secondary amine groups to be abundantly present in the porous structure and to act as mercury receptors. Importantly, the response of TFPPy-CHYD towards Hg^{2+} is very fast and equilibrium is achieved within 2 s. The uniform channel structure of the COFs, results in rapid diffusion of Hg^{2+} and facilitates detection and removal of Hg^{2+}. Thermogravimetric analysis and FT-IR spectra of the COFs indicated excellent thermal and chemical stability.

These unique COFs can also detect and remove other metal ions, such as Pb^{2+}, Cr^{3+}, Cu^{2+}, *etc.* In 2021, Yuan and co-workers reported a new class of 2D COFs (XB-COFs) featuring allyl functionalized hydrazones for the selective and sensitive detection of Pd^{2+} ions through fluorescence signaling (Fig. 23b).[157] The inherent stability of the hydrazone bond and the exceptional complexation ability of allyl towards Pd^{2+} are instrumental in the high-performance fluorescence sensing exhibited by XB-COFs. Notably, XB-COFs exhibit excellent sensing ability across a broad range of pH values, with Pd^{2+} adsorption capacity reaching an impressive 120 mg g^{-1} (Fig. 23c). An increase in fluorescence intensity for XB-COF in solution due to interaction of the Pd^{2+} ions with the allyl of XB-COF, results in high sensitivity with a limit of detection of 0.29 μM. In addition, due to the widespread use of nuclear power and the improper treatment of nuclear waste and accidents, large amounts of radioactive ions have escaped into the environment.[158] Making the exploration of the detection and removal of radioactive ions by COFs an important area of research. In 2020, Qiu and co-workers first developed a cyano-based COF (TFPT-BTAN) by using 2,4,6-tris(4-formylphenyl)-1,3,5-triazine (TFPT) and 2,2′,2″-(benzene-1,3,5-triyl)triacetonitrile (BTAN) and then integrated triazine-based building blocks with amidoxime (AO)-substituted linkers to obtain a fluorescent sp^2 carbon-conjugated COF (TFPT–BTAN–AO) for detecting and removing UO_2^{2+}.[159] TFPT–BTAN–AO exhibited a UO_2^{2+} adsorption capacity of 427 mg g^{-1} and a fast response time with a UO_2^{2+} detection limit of 6.7 nM (Fig. 23d). This COF exhibited good luminescence and chemical and thermal stability. Furthermore, the COF exhibited a high selectivity for UO_2^{2+} because of the introduction of the amidoxime functional group in the open one-dimensional channel of the COF. More importantly, unlike previous COF adsorbents TFPT–BTAN–AO used a very stable carbon–carbon

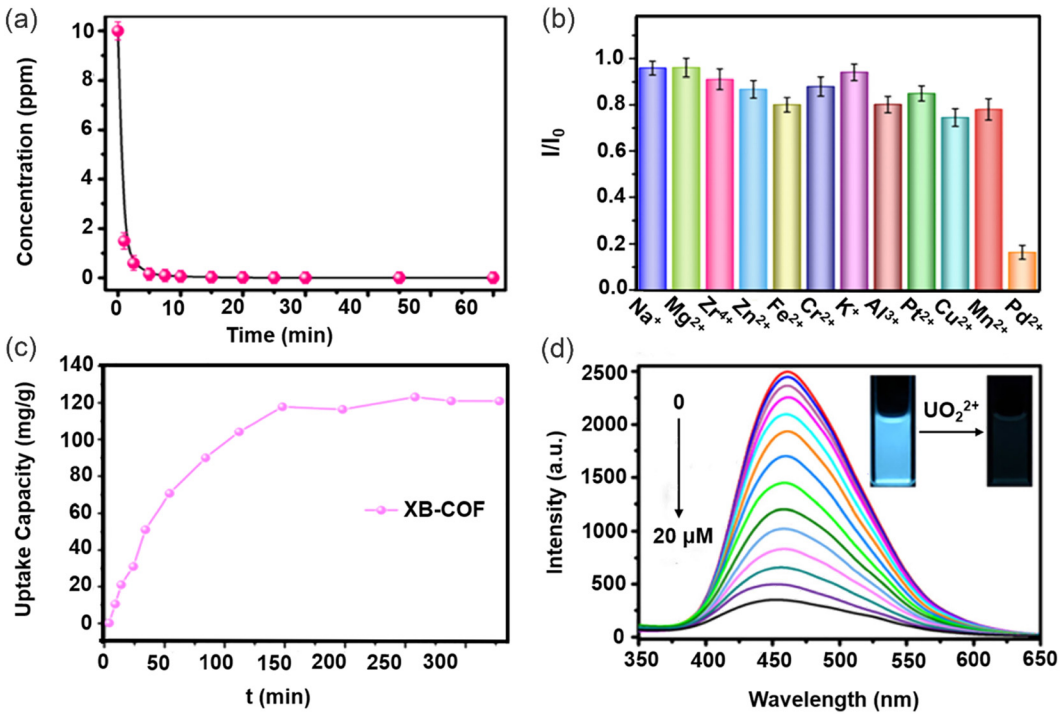

Fig. 23 COFs linkers with high sensitivity and fluorescence efficiency. (a) Adsorption kinetics of Hg^{2+} with TFPPy-CHYD. Reproduced from ref. 156 with permission from American Chemical Society. Copyright 2020. (b) Fluorescence response of XB-COF in presence of different metal ions. (c) Adsorption curves of XB-COF for Pd^{2+}. Reproduced from ref. 157 with permission from American Chemical Society. Copyright 2021. (d) Fluorescence spectra of TFPT–BTAN–AO under different concentrations of UO_2^{2+}. Reproduced from ref. 159 with permission from Springer Nature. Copyright 2020.

double bond, which ensures excellent stability of the COFs and the high adsorption capacity of TFPT–BTAN–AO for UO_2^{2+}.

In conclusion, COFs materials are porous, stable, and have a large adsorption capacity since it is possible to easily introduce specific functional groups to interact with heavy metal ions. The aforementioned benefits render COFs a highly attractive candidate for heavy metal ions sensing and removal applications.[148] In addition, COFs with ligand sites can serve as supramolecular ligands and carriers to further enhance the functions of COFs-based materials. However, the structure of 3D COFs is complex and the synthetic conditions of COFs are limited. Therefore, these characteristics need to be improved to further enhance the functionality of COF-based materials.

4.2. MOF-based materials

Metal organic frameworks (MOFs), a type of porous crystalline material that can be self-assembled through the coordination of metal ions or clusters with organic ligands, have attracted significant attention in recent years.[160–162] MOFs have the advantages of abundant internal surface area, chemical tunability and selective adsorption of a large number of guests,[163,164] allowing MOFs to simultaneously detect and adsorb heavy metal ions in water. For the adsorption of heavy metal ions, MOFs can be regulated by channel functionalization, using a variety of ligands to derive abundant adsorption sites, giving MOFs the capacity to selectively adsorb heavy metal ions in significant amounts. Similar to COFs, MOFs share the same interaction sites for heavy metal ions during the processes of detection and removal. Furthermore, by functionalizing their channels and tuning the pore sizes as well as utilizing diverse ligands, MOFs can acquire abundant adsorption sites and exhibit selective adsorption capabilities towards various heavy metal ions.[165]

Effective fluorescence detection and adsorption of heavy metals ions depends on the selectivity and sensitivity of MOFs. The chelating sites are provided by the MOFs surface groups to facilitate the adsorption of heavy metal ions. For example, Li and co-workers designed and prepared a series of isoreticular luminescent metal–organic frameworks (LMOFs) with Zn-based architectures that incorporate a variety of co-linkers exhibiting diverse functionalities (Fig. 24a).[166] Among them, LMOF-263 exhibits good water stability, high porosity and strong luminescence, with an impressive adsorption capacity for Hg^{2+} of 380 mg g^{-1}, the detection limit for Hg^{2+} was determined to be 3.3 ppb and 19.7 ppb for Pb^{2+}. LMOF-263 has a high quantum yield (89.2%) and a BET surface area of 1004 m^2 g^{-1}, indicating that it can be used as a highly sensitive and selective sensor capable of detecting heavy metal ions in water. Due to the selective interaction of sulfur and oxygen atoms with Hg^{2+} in LMOF-263, the removal rate of Hg^{2+} can reach 99.6% (Fig. 24b). However, when LMOF-263 is recycled, its structure shows signs of degradation, indicating the limited water stability of MOFs. Previously, only few MOFs have shown such high performance in detecting and capturing Hg^{2+} from aqueous solution. Wang and co-workers synthesized a scalable and cost-effective fluorescent MIL-101-NH_2 using a simple one-step method (Fig. 24c).[167] MIL-101-NH_2 exhibited fluorescence detection limits of 0.0018 mM for Fe^{3+}, 0.0016 mM for Cu^{2+} and 0.0052 mM for Pb^{2+} (Fig. 24d). The amino group of the MOFs chelates with metal ions to induce

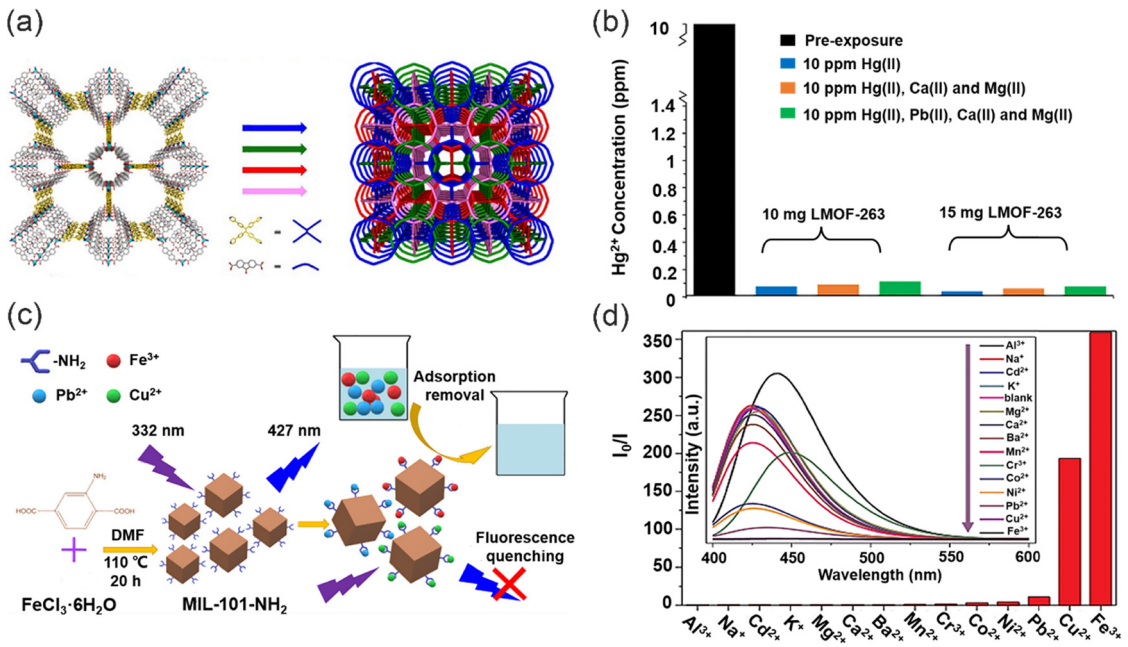

Fig. 24 The structure and chelating sites of MOFs interact with heavy metal ions for the detection and adsorption of heavy metal ions. (a) Isoreticular luminescent metal–organic frameworks with Zn-based architectures. (b) The variation of Hg^{2+} concentrations for various amounts of LMOF-263 in mixed metal solutions. Reproduced from ref. 166 with permission from American Chemical Society. Copyright 2016. (c) The detection and removal of heavy metal ions by MIL-101-NH_2. (d) Fluorescence response of MIL-101-NH_2 towards various metal ions. Reproduced from ref. 167 with permission from Elsevier B.V. Copyright 2019.

host–guest electron transfer, leading to fluorescence quenching, providing the high selectivity and sensitivity of MIL-101-NH_2 for metal ion detection. MIL-101-NH_2 possesses abundant amino groups on its surface, which serve as multiple chelating sites to interact with heavy metal ions, thereby facilitating the efficient adsorption of Fe^{3+}, Cu^{2+} and Pb^{2+}, the adsorption capacities for Fe^{3+}, Cu^{2+} and Pb^{2+} were 3.5, 0.9 and 1.1 mM g^{-1} respectively. Moreover, Wang and co-workers developed an integrated electrode approach using sulfur-functionalized Zr-2,5-dimercaptobenzoic acid metal-organic frameworks (Zr-DMBD-MOFs) and coupled them with a three-dimensional microporous carbon (3D-KSC).[168] This innovative architecture not only facilitated the efficient removal and detection of Hg^{2+} but also enhanced the detection sensitivity. The uniform dispersion of abundant Zr-DMBD-MOFs onto the interconnected framework of 3D-KSC, coupled with the presence of numerous thiol functional groups within the porous Zr-DMBD-MOFs, facilitated the selective enrichment of Hg^{2+} ions on the electrode surface. Significantly, this strategy eliminated potential interference from coexisting heavy metal ions, enabling accurate and precise detection of Hg^{2+} with a detection limit of 0.05 μM. This pioneering work highlights the potential of the Zr-DMBD-MOFs/3D-KSC integrated electrode as a promising platform for the sensitive and selective detection of Hg^{2+} ions, thus addressing a crucial need in environmental monitoring and remediation.

Core–shell MOF@MOF materials, synthesized by combining two MOFs, can integrate different characteristics and functionalities of individual MOFs, providing new functionalities to MOF@MOF structures. Wang and co-workers developed a novel NH_2-MIL-101(Al)@ZIF-8 material with a unique core–shell nanoflower architecture by controlling the intramolecular nucleation and crystal growth processes through the regulation of polyvinylpyrrolidone (PVP) (Fig. 25a).[169] The large specific surface area (1736.257 m^2 g^{-1}), substantial porosity (0.584 cm^3 g^{-1}), and uniformity in pore size (1.5 nm) of NH_2-MIL-101(Al)@ZIF-8 contribute to its physical adsorption ability and enhance the adsorption performance. Significantly, the adsorption of Cu^{2+} on the material takes place *via* monolayer chemisorption between Cu^{2+} and the evenly distributed active sites on the material surface, while the adsorption capacity for Hg^{2+} can reach 459.52 mg g^{-1}. Furthermore, the adsorption and detection abilities are both improved by the synergistic effect of NH_2-MIL-101(Al)@ZIF-8, where the detection ability for Cu^{2+} was as low as 0.17 nM (Fig. 25b).

To further improve the sensitivity and adsorption capacity of MOFs for heavy metal ions. In 2020, Sewify and co-workers developed thioketone Al-MOFs monitors (TAM) *via* the direct immobilization of the chromophore on to the microporous surface of Al-MOFs.[170] With the addition of Hg^{2+}, a new absorption peak (λ = 600 nm) appeared (Fig. 25d) and the sensor exhibits a detection limit of 0.8 × 10^{-3} ppm for Hg^{2+} ions and can reach an adsorption capacity of 1110 mg g^{-1} for Hg^{2+} (Fig. 25c). Since organic receptors can be directly immobilized on to the microporous MOF backbone, real-time monitoring efficiency and sensitivity can be improved. Moreover, in the presence of Hg^{2+}, the measured absorption spectra were

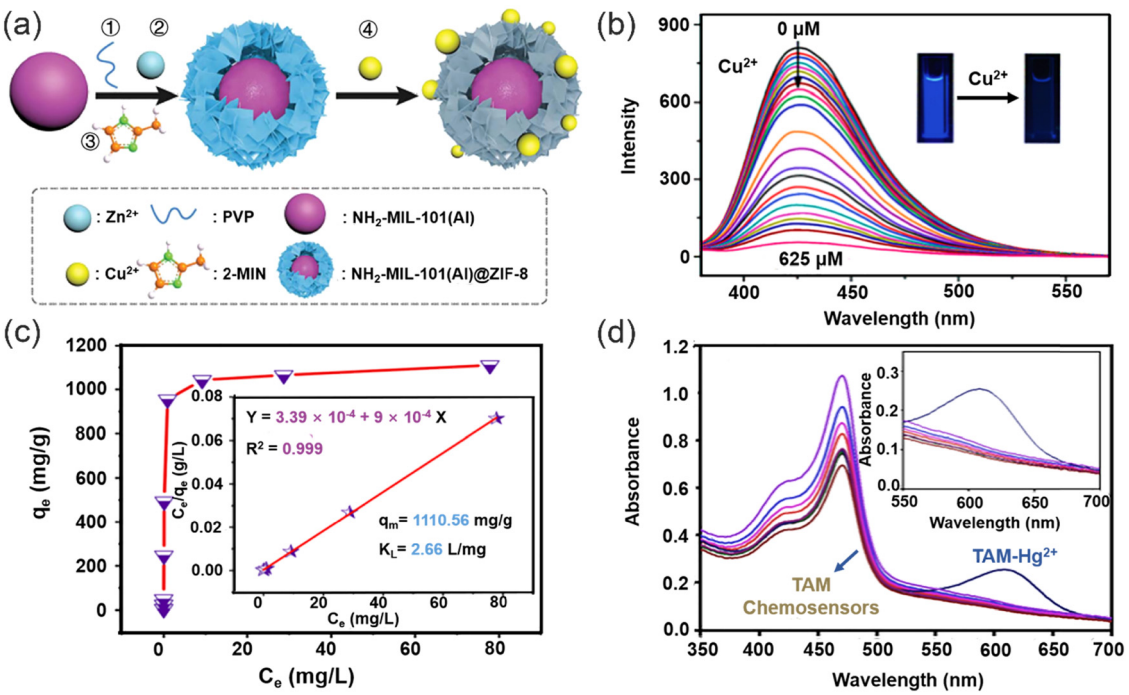

Fig. 25 Fluorescence response and removal of heavy metal ions by MOFs with different structures. (a) The synthesis of core–shell NH_2-MIL-101(Al)@ZIF-8 nanoflowers for the simultaneous detection and removal of Cu^{2+} ions. (b) Fluorescence spectra of the NH_2-MIL-101(Al)@ZIF-8 suspension with the addition of various concentrations of Cu^{2+}. Reproduced from ref. 169 with permission from Royal Society of Chemistry. Copyright 2018. (c) Langmuir isotherm and the linear relation inset for removal of Hg^{2+}. (d) Effect of Hg^{2+} on absorbance spectra of TAM chemosensors. Reproduced from ref. 170 with permission from American Chemical Society. Copyright 2020.

significantly enhanced compared to other metal ions, confirming the superior selectivity of the Al-MOFs for Hg^{2+}. In 2021, Safaei and co-workers developed a fluorescent MOF, $[Zn_2(DpTzTz)_2\ (BDC)_2]\cdot 2DMF$, which was composed of Zn^{2+}, 2,5-di(4-pyridyl)thiazolo[4,5-ɒ]thiazole (DpTzTz), and terephthalic acid. Due to the strong chelating sites of DpTzTz for mercury ions, the $[Zn_2(DpTzTz)_2\ (BDC)_2]\cdot 2DMF$ exhibits exceptional removal capability with an adsorption capacity of up to 1428 mg g^{-1}.[171] Furthermore, coordination of Hg^{2+} with the sulfur and nitrogen atoms indicates that the incorporation of the rigid conjugated thiazolothiazole (TzTz) functional group, containing Lewis basic nitrogen and sulfur atoms, into the MOF is able to enhance host–guest interactions with Hg^{2+}, enabling the MOF to detect and remove Hg^{2+}.

In conclusion, due to their remarkable properties, including high surface area, large pore size, and abundant adsorption sites, MOFs exhibit great potential for both detecting and removing heavy metal ions with high efficiency. However, future research should be directed towards improving the rate that MOFs can adsorb heavy metal ions from water. Additionally, previous research has shown that the introduction of carbon dots into COF and MOF matrices can enhance their luminescent properties.[172,173] The introduction of carbon dots into MOF or COF matrices not only facilitates structural modifications but also serves as a surface modifier, reducing surface defects in the materials, thereby enhancing the optical stability of the composite.[174–176] However, although the introduction of carbon dots can improve the luminescent properties, there is still scope for improvement in terms of detection sensitivity and adsorption capacity.

4.3. Porous silica materials

Porous silica is a silica material consisting of interconnected channels and pores with unique properties.[177] The shape, size, and distribution of these channels and pores can be precisely controlled through various fabrication methods and processing conditions. Previous research has demonstrated that by immobilizing organic ligands onto mesoporous silica, composite materials can be formed, exhibiting unique properties.[178,179] These organic ligands possess selective adsorption and high dispersion capabilities, which combined with the high specific surface area and excellent chemical stability of mesoporous silica,[180] enable the composite material to interact with heavy metal ions and other metal ions (Fig. 26).[181–183] Therefore, these composite materials exhibit tremendous potential for the detection and adsorption of heavy metal ions.

Mesoporous silica is a porous silicon dioxide material with a highly ordered pore structure.[184] The hydroxyl groups on its surface can be used to anchor functional organic ligands onto mesoporous silica through reversible covalent bonds and non-covalent interactions such as hydrogen bonding, enabling the detection and adsorption of target ions (Fig. 27a). For example, Awual synthesized a functional ligand, *N*,*N*-disalicylidene-4,5-dimethyl-phenylenedene (DDPD), and anchored it onto mesoporous silica for the detection and removal of Cu^{2+} from wastewater.[185] Complexation of Cu^{2+} ions with functional groups from the organic ligand, facilitated the detection of Cu^{2+} ions through naked-eye observation or UV-vis absorption measurements (Fig. 27b), with a detection limit of 0.37 μg L^{-1}. Moreover, the immobilization of the organic ligand within highly ordered mesoporous silica provides additional active sites for the interaction between the DDPD material and Cu^{2+} ions. The structure of mesoporous silica also enhances the adsorption capacity of the composite material for Cu^{2+}, with a maximum adsorption capacity of 183.81 mg g^{-1}. Similarly, in 2023, Awual and co-workers impregnated mesoporous silica with *N*,*N*-bis(salicylidene)1,2-bis(2-aminophenylthio) ethane (BSBAE), resulting in an optical composite material (OCM) for the detection and removal of Cd^{2+}.[186] Due to the non-covalent

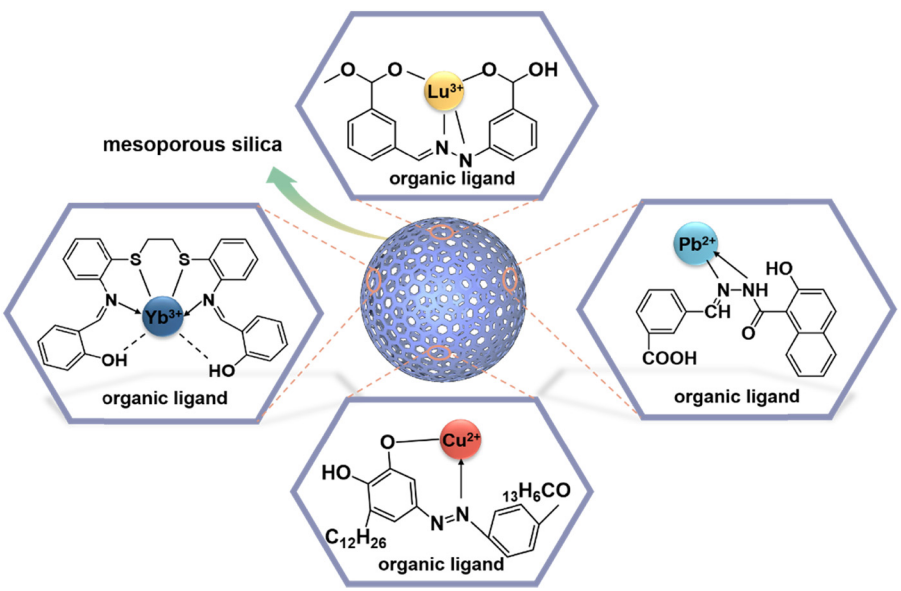

Fig. 26 Mechanism of interactions between mesoporous silica and metal ions.

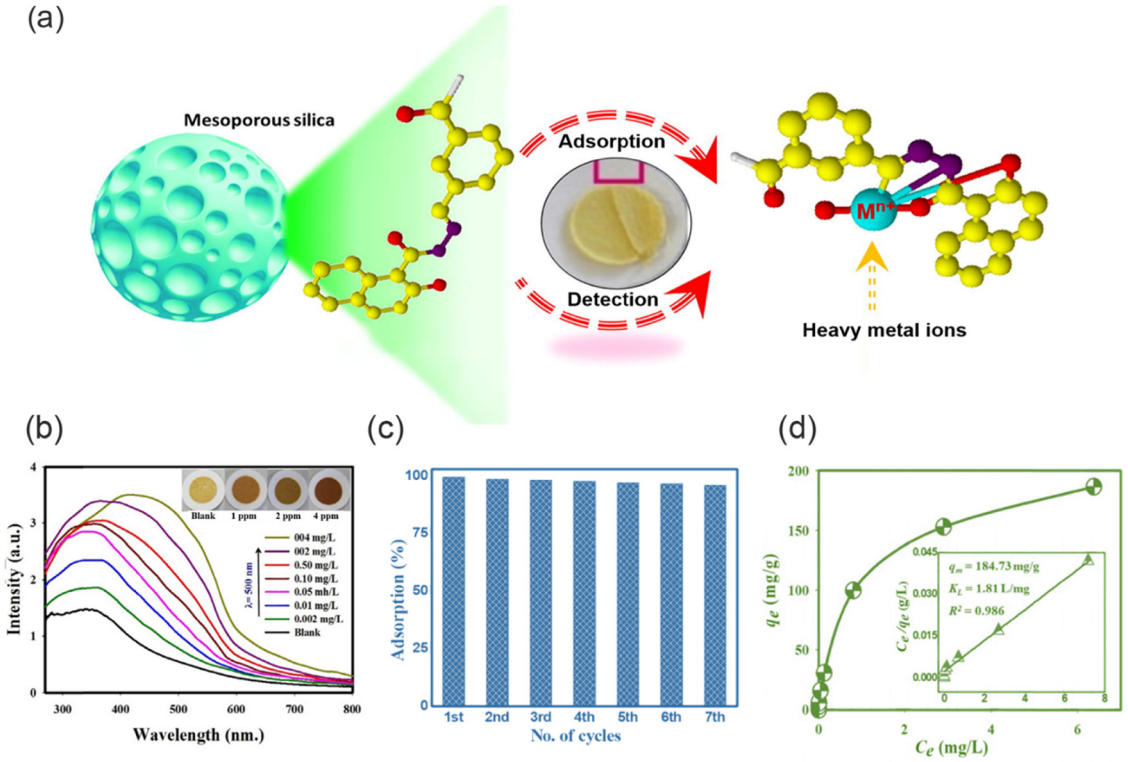

Fig. 27 Mechanism of mesoporous silica materials for the detection and removal of heavy metal ions. (a) The mechanism of action of the organic ligand in mesoporous silica. Reproduced from ref. 187 with permission from Elsevier B.V. Copyright 2021. (b) The sensitivity of the composite material at different concentrations of Cu^{2+}. Reproduced from ref. 185 with permission from Elsevier B.V. Copyright 2016. (c) Recycling efficiency of optical composite material. Reproduced from ref. 186 with permission from Elsevier B.V. Copyright 2022. (d) Langmuir isotherm and the linear relation inset for removal of Cu^{2+}. Reproduced from ref. 188 with permission from Elsevier B.V. Copyright 2023.

interaction between the hydroxyl groups of the mesoporous silica and the BSBAE ligand, as well as the presence of van der Waals forces and reversible covalent bonds, the OCM can interact with Cd^{2+} ions without disrupting the original structure of mesoporous silica. Furthermore, effective desorption of Cd^{2+} from the OCM was achieved using HCl, with a desorption efficiency of up to 99%. The OCM exhibited a high recyclability after being rinsed with water (Fig. 27c), highlighting one of the main advantages of mesoporous silica composite materials.

In addition to enabling effective detection and adsorption of heavy metal ions through the incorporation of specific functional groups, further enhancement of detection sensitivity and adsorption capacity of mesoporous silica materials can be achieved through the optimization of the fabrication methods and material processing.[187] For example, Salman and co-workers immobilized the functional organic ligand, 4-*tert*-octyl-4-((phenyl)diazenyl)phenol, onto mesoporous silica to prepare a composite adsorbent.[188] Then by adjusting the pH, a lower detection limit of 0.28 μg L^{-1} and an increased maximum adsorption capacity of 184.7 mg g^{-1} for Cu^{2+} by the material was achieved (Fig. 27d). The pore size, porosity, and surface charge of mesoporous silica may vary under different pH conditions, which can influence the interactions between the mesoporous silica materials and Cu^{2+}. Therefore, optimizing the pH is crucial to achieve the best detection and adsorption performance.

In conclusion, mesoporous silica composite materials exhibit several advantages such as selective adsorption, high adsorption capacity, and recyclability, rendering them highly promising for applications in environmental monitoring and wastewater treatment. Furthermore, the stability of mesoporous silica can be further enhanced, and its adsorption performance can be improved by employing diverse functional group modification strategies and optimizing the structure.

5. Conclusions and perspectives

5.1. Conclusions

In summary, this review provides an overview of recent advancements in the field of advanced functional materials, specifically chromophore-based functional materials, for the detection and removal of heavy metal ions. Based on the synergistic interplay between the chromophores and substrate materials such as polymers and porous materials, the advanced functional materials developed exhibit superior performance for heavy metal ion detection and removal compared to conventional materials. Various types of chromophores endow the substrate materials with excellent heavy metal ion recognition capabilities, outstanding mechanical properties, and enhanced efficiency in metal removal. Meanwhile, the distinctive structure of the substrate materials contributes to the increased

stability and environmental sustainability of the chromophores. Through an in-depth analysis of the reviewed work, it is evident that a wide range of sophisticated platforms have been developed to meet the increasing demand for efficient detection and removal of diverse heavy metal ion contaminants. The cutting-edge technologies and innovative strategies discussed in this review have led to remarkable progress in the design of functional materials that are not only convenient, stable, and rapid but also sensitive, environmentally friendly, and recyclable. These materials exhibit great potential for precise detection, even at ultra-low detection limits, and efficient removal of heavy metal ions. The advancements in selectivity and adsorption capacity have significantly enhanced the overall efficiency and practicability of heavy metal ion detection and removal processes. The integration of chromophores with polymers and porous materials, utilizing optical detection and chemisorption methods, has emerged as a promising approach for the treatment of various heavy metal ions pollutants. However, it is important to acknowledge that certain challenges still need to be overcome. Most functional materials can only detect and adsorb specific heavy metal ions. However, wastewater often contains a mixture of heavy metal ions, and the competitive adsorption among them can affect the removal efficiency of functional materials towards specific heavy metal ions. Furthermore, the concept of utilizing functional materials for the simultaneous detection and removal of heavy metal ions is still in its infancy. The preparation and use of these materials involves complex steps, making them unsuitable for real-world wastewater treatment. Although current functional materials exhibit the capability to accomplish these dual tasks, the detection efficiency of these bifunctional materials may not match that of dedicated sensor materials, and their adsorption capacity may be limited compared to conventional adsorbent materials. Moreover, actual wastewater is in a flowing state, and continuous flow can exert a level of "wear and tear" on the materials, leading to damage. Meanwhile, most exhausted functional materials are disposed of by being buried or incinerated, leading to a potential threat to the environment. As such, significant additional research should focus on improving the selectivity, stability of materials towards the detection and removal of heavy metal ions as well as maintaining their sustainability and cost-effectiveness.

5.2. Perspectives

The integration of chromophore-based sensors with polymers and porous materials displays significant potential and while remarkable progress has been made for the treatment of heavy metal ion pollution, the sensing and extraction systems are still at an early stage and critical challenges remain, which restricts their further utility in real world applications. These novel heavy metal ion detection and removal systems based on functional materials still need to be improved to provide: (i) enhanced sensing and extraction ability: the systems should be capable of detecting heavy metal ions sensitively in a stable and constant manner, facilitating the detection in drinking water. In addition, among all the heavy metal ions, the coexistence of some cations such as Cd^{2+}, Pb^{2+}, Cu^{2+}, Cr^{6+} and Hg^{2+} results in a decrease in the adsorption capacity of the functional material for the target heavy metal ions due to competing adsorption. Therefore, the design of highly selective materials is required which could be achieved by decorating the materials with additional multifunctional groups; (ii) Increasing the stability: although some systems based on non-covalent bonding have been developed for the detection and removal of heavy metal ions, the stability of systems based on non-covalent bonding is susceptible to environmental factors such as temperature and pH when compared to more stable covalent bonding systems. Therefore, the development of more stable systems for the detection and removal of heavy metal ions should be further investigated; (iii) multifunctional systems: most of the prepared systems can only detect or remove a single heavy metal ion, and when multiple heavy metal ions coexist, the detection and removal abilities are reduced, which limits their development for practical applications. Therefore, the rational design of systems capable of detecting and removing various heavy metal ions simultaneously is required to meet the needs of practical systems; (iv) enhanced mechanical performance: the treatment of wastewater necessitates the implementation of continuous flow processes, demanding materials with extraordinary mechanical properties that are well-suited for such applications. Achieving the requisite mechanical stability under dynamic flowing conditions is essential to withstand the high velocities inherent in wastewater treatment. (v) Appropriate dimensions: thicker materials excel in removal efficiency but have reduced sensing capability, while thinner materials exhibit exceptional sensing performance but lower adsorption capacity. As such, precise structural design is essential to achieve enhanced detection and removal of heavy metal ions. (vi) Hybrid design strategy: designs that couple a film detection layer with an adsorbent material layer to achieve high-efficiency detection and adsorption. (vii) Sustainability: eco-friendly materials are required to facilitate the development of green chemistry practices. Recyclable and degradable materials like cellulose, chitosan and lignin have attracted great interest due to their abundance in nature and they are cheap and readily available. Systems constructed based on these materials for the simultaneous detection and removal of heavy metal ions possessing outstanding stability and reusability are superior to other common materials; (viii) smart phone-based on-site analysis systems: traditional laboratory-based analyses, which involves complex sample preparation, specialized personnel and/or expensive instrumentation, are unsuitable for simple and comprehensive environmental monitoring. Therefore, reliable, cost-effective, and easy-to-use multifunctional and portable quantification systems need to be developed; (ix) safe reuse or disposal of used materials: currently, most of the materials are discarded and disposed of after the detection and removal of heavy metal ions. Therefore, to avoid secondary pollution, more advanced disposal or up-cycling methods need to be developed.[189]

As a final thought, although the sensing platforms based on the materials discussed in this review still face many challenges, it is gratifying to note that current research provides hope for the construction of practical systems in the not-too-distant future. Systems with catalytic decontamination abilities are particularly interesting and deserve concerted development, since they have

the ability to convert pollutants to harmless or low toxicity species. In summary we anticipate that with the continuous development of chemical materials and detection strategies, that advanced functional systems will be developed for the treatment of various heavy metal ions enabling improved environmental remediation and clean drinking water for everyone. Such progress is expected to continue in the coming years, enabling us to address the challenges of heavy metal ion contamination with ever increasing efficacy and efficiency.

Conflicts of interest

T. D. J. was a High-Level Foreign Expert of North China Electric Power University during the preparation of this review.

Acknowledgements

This research is supported by the National Natural Science Foundation of China (No. 21607044, 51878273), and the Fundamental Research Funds for the Central Universities (No. 2023MS146). T. D. J. wishes to thank the Royal Society for a Wolfson Research Merit Award and the Open Research Fund of the School of Chemistry and Chemical Engineering, Henan Normal University for support (2020ZD01).

References

1 S. Bolisetty, M. Peydayesh and R. Mezzenga, *Chem. Soc. Rev.*, 2019, **48**, 463–487.
2 C. F. Carolin, P. S. Kumar, A. Saravanan, G. J. Joshiba and M. Naushad, *J. Environ. Chem. Eng.*, 2017, **5**, 2782–2799.
3 D. J. Sarkar, S. Das Sarkar, B. K. Das, B. K. Sahoo, A. Das, S. K. Nag, R. K. Manna, B. K. Behera and S. Samanta, *Water Res.*, 2021, **192**, 116853.
4 K. Vikrant and K.-H. Kim, *Chem. Eng. J.*, 2019, **358**, 264–282.
5 R. Li, H. Wu, J. Ding, W. Fu, L. Gan and Y. Li, *Sci. Rep.*, 2017, **7**, 46545.
6 A. B. Tabrizi, *J. Hazard. Mater.*, 2007, **139**, 260–264.
7 M. R. Awual, M. Ismael, T. Yaita, S. A. El-Safty, H. Shiwaku, Y. Okamoto and S. Suzuki, *Chem. Eng. J.*, 2013, **222**, 67–76.
8 C. Liu, R. Bai and Q. S. Ly, *Water Res.*, 2008, **42**, 1511–1522.
9 Y. Al-Degs, M. A. M. Khraisheh and M. F. Tutunji, *Water Res.*, 2001, **35**, 3724–3728.
10 H. N. Kim, W. X. Ren, J. S. Kim and J. Yoon, *Chem. Soc. Rev.*, 2012, **41**, 3210–3244.
11 C. Guo and J. Irudayaraj, *Anal. Chem.*, 2011, **83**, 2883–2889.
12 M. K. Nazeeruddin, D. Di Censo, R. Humphry-Baker and M. Gratzel, *Adv. Funct. Mater.*, 2006, **16**, 189–194.
13 G. H. Chen, *Sep. Purif. Technol.*, 2004, **38**, 11–41.
14 M. Li, N. Chen, H. Shang, C. Ling, K. Wei, S. Zhao, B. Zhou, F. Jia, Z. Ai and L. Zhang, *Environ. Sci. Technol.*, 2022, **56**, 10945–10953.
15 S. Su, B. Chen, M. He and B. Hu, *Talanta*, 2014, **123**, 1–9.
16 F. A. Aydin and M. Soylak, *J. Hazard. Mater.*, 2010, **173**, 669–674.
17 T. G. Kazi, N. Jalbani, M. B. Arain, M. K. Jamali, H. I. Afridi, R. A. Sarfraz and A. Q. Shah, *J. Hazard. Mater.*, 2009, **163**, 302–307.
18 M. Tüzen, *Food Chem.*, 2003, **80**, 119–123.
19 Y. Fang, Y. Zhang, L. Cao, J. Yang, M. Hu, Z. Pang and J. He, *ACS Appl. Mater. Interfaces*, 2020, **12**, 11761–11768.
20 T. Kondo, W. J. Chen and G. S. Schlau-Cohen, *Chem. Rev.*, 2017, **117**, 860–898.
21 E. M. Nolan and S. J. Lippard, *Chem. Rev.*, 2008, **108**, 3443–3480.
22 R. Freeman, T. Finder and I. Willner, *Angew. Chem., Int. Ed.*, 2009, **48**, 7818–7821.
23 Z.-H. Lin, G. Zhu, Y. S. Zhou, Y. Yang, P. Bai, J. Chen and Z. L. Wang, *Angew. Chem., Int. Ed.*, 2013, **52**, 5065–5069.
24 C. Zhao, G. Liu, Q. Tan, M. Gao, G. Chen, X. Huang, X. Xu, L. Li, J. Wang, Y. Zhang and D. Xu, *J. Adv. Res.*, 2023, **44**, 53–70.
25 E. S. Dragan, *Chem. Eng. J.*, 2014, **243**, 572–590.
26 E. A. Gendy, J. Ifthikar, J. Ali, D. T. Oyekunle, Z. Elkhlifia, I. I. Shahib, A. I. Khodair and Z. Chen, *J. Environ. Chem. Eng.*, 2021, **9**, 105687.
27 M. Hasan, M. A. Shenashen, M. N. Hasan, H. Znad, M. S. Salman and R. Awual, *J. Mol. Liq.*, 2021, **323**, 114587.
28 M. S. Salman, M. N. Hasan, K. T. Kubra and M. M. Hasan, *Microchem. J.*, 2021, **162**, 105868.
29 B. Ramalingam, T. Parandhaman, P. Choudhary and S. K. Das, *ACS Sustainable Chem. Eng.*, 2018, **6**, 6328–6341.
30 S. Biswas and R. Biswas, *Chemosphere*, 2023, **312**, 137187.
31 L. Zhou, Y. Lin, Z. Huang, J. Ren and X. Qu, *Chem. Commun.*, 2012, **48**, 1147–1149.
32 T. Liu, J. X. Dong, S. G. Liu, N. Li, S. M. Lin, Y. Z. Fan, J. L. Lei, H. Q. Luo and N. B. Li, *J. Hazard. Mater.*, 2017, **322**, 430–436.
33 L. Wang, Y. Wang, W. Li, W. Zhi, Y. Liu, L. Ni and Y. Wang, *ACS Appl. Mater. Interfaces*, 2019, **11**, 40575–40584.
34 W. Wang, N.-K. Wong, M. Sun, C. Yan, S. Ma, Q. Yang and Y. Li, *ACS Appl. Mater. Interfaces*, 2015, **7**, 8868–8875.
35 K. T. Kubra, M. S. Salman, H. Znad and M. N. Hasan, *J. Mol. Liq.*, 2021, **329**, 115541.
36 M. R. Awual, M. N. Hasan, M. M. Hasan, M. S. Salman, M. C. Sheikh, K. T. Kubra, M. S. Islam, H. M. Marwani, A. Islam, M. A. Khaleque, R. M. Waliullah, M. S. Hossain, A. I. Rasee, A. I. Rehan and M. E. Awual, *Sep. Purif. Technol.*, 2023, **319**, 124088.
37 M. S. Salman, M. C. Sheikh, M. M. Hasan, M. N. Hasan, K. T. Kubra, A. I. Rehan, M. E. Awual, A. I. Rasee, R. M. Waliullah, M. S. Hossain, M. A. Khaleque, A. K. D. Alsukaibi, H. M. Alshammari and M. R. Awual, *Appl. Surf. Sci.*, 2023, **622**, 157008.
38 A. Islam, S. H. Teo, Y. H. Taufiq-Yap, C. H. Ng, D.-V. N. Vo, M. L. Ibrahim, M. M. Hasan, M. A. R. Khan, A. S. M. Nur and M. R. Awual, *Resour. Conserv. Recy.*, 2021, **175**, 105849.
39 M. T. Chorsi, E. J. Curry, H. T. Chorsi, R. Das, J. Baroody, P. K. Purohit, H. Ilies and T. D. Nguyen, *Adv. Mater.*, 2019, **31**, 1802084.
40 D. Zhang, Q. Chen, C. Shi, M. Chen, K. Ma, J. Wan and R. Liu, *Adv. Funct. Mater.*, 2021, **31**, 2007226.

41 B. K. Rani and S. A. John, *J. Hazard. Mater.*, 2018, **343**, 98–106.
42 S.-Y. Yu and S.-P. Wu, *Sens. Actuators, B*, 2014, **201**, 25–30.
43 J. Luo, Z. Xie, J. W. Lam, L. Cheng, H. Chen, C. Qiu, H. S. Kwok, X. Zhan, Y. Liu and D. J. C. C. Zhu, *Chem. Commun.*, 2001, 1740–1741.
44 W.-M. Wang, D. Dai, J.-R. Wu, C.-Y. Wang, Y. Wang and Y.-W. Yang, *Chem. – Eur. J.*, 2021, **27**, 11879–11887.
45 H.-F. Xie, C.-J. Yu, Y.-L. Huang, H. Xu, Q.-L. Zhang, X.-H. Sun, X. Feng and C. Redshaw, *Mater. Chem. Front.*, 2020, **4**, 1500–1506.
46 K. Rout, A. K. Manna, M. Sahu, J. Mondal, S. K. Singh and G. K. Patra, *RSC Adv.*, 2019, **9**, 25919–25931.
47 B. Yuan, D.-X. Wang, L.-N. Zhu, Y.-L. Lan, M. Cheng, L.-M. Zhang, J.-Q. Chu, X.-Z. Li and D.-M. Kong, *Chem. Sci.*, 2019, **10**, 4220–4226.
48 N. Sinha, L. Stegemann, T. T. Y. Tan, N. L. Doltsinis, C. A. Strassert and F. E. Hahn, *Angew. Chem., Int. Ed.*, 2017, **56**, 2785–2789.
49 D. Qi, J. Zhang, D. Zhang, M. Zhu, L. Gong, C. Su, W. Lu, Y. Bian and J. Jiang, *Dyes Pigm.*, 2020, **173**, 107941.
50 Y. Chen, W. Zhang, Y. Cai, R. T. K. Kwok, Y. Hu, J. W. Y. Lam, X. Gu, Z. He, Z. Zhao, X. Zheng, B. Chen, C. Gui and B. Z. Tang, *Chem. Sci.*, 2017, **8**, 2047–2055.
51 K. Gupta, P. Joshi, R. Gusain and O. P. Khatri, *Coord. Chem. Rev.*, 2021, **445**, 214100.
52 R. Bhateria and R. Singh, *J. Water Process Eng.*, 2019, **31**, 100845.
53 R. Baby, B. Saifullah and M. Z. Hussein, *Nanoscale Res. Lett.*, 2019, **14**, 1–17.
54 R. Gusain, N. Kumar and S. S. Ray, *Coord. Chem. Rev.*, 2020, **405**, 213111.
55 N. Bhardwaj and S. C. Kundu, *Biotechnol. Adv.*, 2010, **28**, 325–347.
56 D. Chen, K. Jiang, T. Huang and G. Shen, *Adv. Mater.*, 2020, **32**, 1901806.
57 G. Aragay, J. Pons and A. Merkoci, *Chem. Rev.*, 2011, **111**, 3433–3458.
58 E. Vunain, A. K. Mishra and B. B. Mamba, *Int. J. Biol. Macromol.*, 2016, **86**, 570–586.
59 J. Y. Lim, N. M. Mubarak, E. C. Abdullah, S. Nizamuddin, M. Khalid and Inamuddin, *J. Ind. Eng. Chem.*, 2018, **66**, 29–44.
60 X. Wang, Z.-J. Liu, E. H. Hill, Y. Zheng, G. Guo, Y. Wang, P. S. Weiss, J. Yu and Y.-W. Yang, *Matter*, 2019, **1**, 848–861.
61 X. Chen and S. S. Mao, *Chem. Rev.*, 2007, **107**, 2891–2959.
62 H. Li, D.-X. Chen, Y.-L. Sun, Y. B. Zheng, L.-L. Tan, P. S. Weiss and Y.-W. Yang, *J. Am. Chem. Soc.*, 2013, **135**, 1570–1576.
63 H. Li, L.-L. Tan, P. Jia, Q.-L. Li, Y.-L. Sun, J. Zhang, Y.-Q. Ning, J. Yu and Y.-W. Yang, *Chem. Sci.*, 2014, **5**, 2804–2808.
64 R. Deng, N. Shen, Y. Yang, H. Yu, S. Xu, Y.-W. Yang, S. Liu, K. Meguellati and F. Yan, *Biomaterials*, 2018, **167**, 80–90.
65 S. Chatterjee, X.-Y. Lou, F. Liang and Y.-W. Yang, *Coord. Chem. Rev.*, 2022, **459**, 214461.
66 Q. Niu, P. Gao, M. Yuan, G. Zhang, Y. Zhou, C. Dong, S. Shuang and Y. Zhang, *Microchem. J.*, 2019, **146**, 1140–1149.
67 Y. Liu, Y. Liu, L. Xu, J. Li, X. Liu, J. Liu and G. Li, *Sens. Actuators, B*, 2017, **249**, 331–338.
68 G. Chen, J. Hai, H. Wang, W. Liu, F. Chen and B. Wang, *Nanoscale*, 2017, **9**, 3315–3321.
69 J. Zhou, H. Zhou, J. Tang, S. Deng, F. Yan, W. Li and M. Qu, *Microchim. Acta*, 2017, **184**, 343–368.
70 P. Zuo, X. Lu, Z. Sun, Y. Guo and H. He, *Microchim. Acta*, 2016, **183**, 519–542.
71 Z. Wang, C. Xu, Y. Lu, X. Chen, H. Yuan, G. Wei, G. Ye and J. Chen, *Sens. Actuators, B*, 2017, **241**, 1324–1330.
72 S. Li, J. Luo, G. Yin, Z. Xu, Y. Le, X. Wu, N. Wu and Q. Zhang, *Sens. Actuators, B*, 2015, **206**, 14–21.
73 E. F. C. Simoes, J. M. M. Leitao and J. C. G. Esteves da Silva, *Microchim. Acta*, 2016, **183**, 1769–1777.
74 T. Hao, X. Wei, Y. Nie, Y. Xu, Y. Yan and Z. Zhou, *Microchim. Acta*, 2016, **183**, 2197–2203.
75 W. Yao, N. Wu, Z. Lin, J. Chen, S. Li, S. Weng, L. Zhang, A. Liu and X. Lin, *Microchim. Acta*, 2017, **184**, 907–914.
76 S. N. Baker and G. A. Baker, *Angew. Chem., Int. Ed.*, 2010, **49**, 6726–6744.
77 H. Li, Z. Kang, Y. Liu and S.-T. Lee, *J. Mater. Chem.*, 2012, **22**, 24230–24253.
78 M. Zheng, Z. Xie, D. Qu, D. Li, P. Du, X. Jing and Z. Sun, *ACS Appl. Mater. Interfaces*, 2013, **5**, 13242–13247.
79 R. Zhang and W. Chen, *Biosens. Bioelectron.*, 2014, **55**, 83–90.
80 Y. Zhai, B. Zhang, R. Shi, S. Zhang, Y. Liu, B. Wang, K. Zhang, G. I. N. Waterhouse, T. Zhang and S. Lu, *Adv. Energy Mater.*, 2022, **12**, 2103426.
81 F. Limosani, E. M. Bauer, D. Cecchetti, S. Biagioni, V. Orlando, R. Pizzoferrato, P. Prosposito and M. Carbone, *Nanomaterials*, 2021, **11**, 2249.
82 J. Zhao, C. Li, X. Du, Y. Zhu, S. Li, X. Liu, C. Liang, Q. Yu, L. Huang and K. Yang, *Small*, 2022, **18**, 2200744.
83 A. Sekar, R. Yadav and N. Basavaraj, *New J. Chem.*, 2021, **45**, 2326–2360.
84 W. Meng, X. Bai, B. Wang, Z. Liu, S. Lu and B. Yang, *Energy Environ. Mater.*, 2019, **2**, 172–192.
85 Y. Liu, Q. Zhou, J. Li, M. Lei and X. Yan, *Sens. Actuators, B*, 2016, **237**, 597–604.
86 Q. Liu, N. Zhang, H. Shi, W. Ji, X. Guo, W. Yuan and Q. Hu, *New J. Chem.*, 2018, **42**, 3097–3101.
87 Z. Ma, H. Ming, H. Huang, Y. Liu and Z. Kang, *New J. Chem.*, 2012, **36**, 861–864.
88 Y. Xie, D. Cheng, X. Liu and A. Han, *Sensors*, 2019, **19**, 3169.
89 Z. Y. Liu, W. Y. Jin, F. X. Wang, T. C. Li, J. F. Nie, W. C. Xiao, Q. Zhang and Y. Zhang, *Sens. Actuators, B*, 2019, **296**, 126698.
90 S. Wen, T. Zeng, L. Liu, K. Zhao, Y. Zhao, X. Liu and H.-C. Wu, *J. Am. Chem. Soc.*, 2011, **133**, 18312–18317.
91 L. Tan, Z. Chen, C. Zhang, X. Wei, T. Lou and Y. Zhao, *Small*, 2017, **13**, 1603370.
92 Y. Li, H. Gao, Z. Qi, Z. Huang, L. Ma and J. Liu, *Angew. Chem., Int. Ed.*, 2021, **60**, 12985–12991.

93 W.-M. Wang, D. Dai, J.-R. Wu, C. Wang, Y. Wang and Y.-W. Yang, *Dyes Pigm.*, 2022, **207**, 110712.
94 D. P. Dubal, N. R. Chodankar, D.-H. Kim and P. Gomez-Romero, *Chem. Soc. Rev.*, 2018, **47**, 2065–2129.
95 H. N. Kim, Z. Guo, W. Zhu, J. Yoon and H. Tian, *Chem. Soc. Rev.*, 2011, **40**, 79–93.
96 D. Dai, J. Yang, Y. Wang and Y. W. Yang, *Adv. Funct. Mater.*, 2020, **31**, 2006168.
97 S. H. Byun, J. W. Chung and S. Y. Kwak, *J. Water Process Eng.*, 2019, **29**, 100757.
98 K. N. Han, B. Y. Yu and S.-Y. Kwak, *J. Membr. Sci.*, 2012, **396**, 83–91.
99 W.-P. Zhu, J. Gao, S.-P. Sun, S. Zhang and T.-S. Chung, *J. Membr. Sci.*, 2015, **487**, 117–126.
100 E. Ferrari, E. Ranucci, U. Edlund and A.-C. Albertsson, *J. Appl. Polym. Sci.*, 2014, **132**, 41695.
101 A. Maleki, B. Hayati, F. Najafi, F. Gharibi and S. W. Joo, *J. Mol. Liq.*, 2016, **224**, 95–104.
102 M. Sajid, M. K. Nazal, Ihsanullah, N. Baig and A. M. Osman, *Sep. Purif. Technol.*, 2018, **191**, 400–423.
103 H. Yoo and S.-Y. Kwak, *J. Membr. Sci.*, 2013, **448**, 125–134.
104 J. Y. Sum, A. L. Ahmad and B. S. Ooi, *J. Membr. Sci.*, 2014, **466**, 183–191.
105 Y.-J. Tang, Z.-L. Xu, B.-Q. Huang, Y.-M. Wei and H. Yang, *RSC Adv.*, 2016, **6**, 45585–45594.
106 M. Li, Z. Liu, S. Wang, D. G. Calatayud, W.-H. Zhu, T. D. James, L. Wang, B. Mao and H.-N. Xiao, *Chem. Commun.*, 2018, **54**, 184–187.
107 H. Shao, D. Yin, D. Li, Q. Ma, W. Yu and X. Dong, *ACS Appl. Mater. Interfaces*, 2021, **13**, 49288–49300.
108 M. Li, X. An, M. Jiang, S. Li, S. Liu, Z. Chen and H. Xiao, *ACS Sustainable Chem. Eng.*, 2019, **7**, 15182–15189.
109 M. Khan and I. M. C. Lo, *J. Hazard. Mater.*, 2017, **322**, 195–204.
110 W. L. Yan and R. B. Bai, *Water Res.*, 2005, **39**, 688–698.
111 M. Li, X. Li, M. Xu, B. Liu, M. Yang, Z. Chen, T. Gao, T. D. James, L. Wang and H. Xiao, *Chem. Eng. J.*, 2021, **426**, 131296.
112 A. Alam, Y. Zhang, H.-C. Kuan, S.-H. Lee and J. Ma, *Prog. Polym. Sci.*, 2018, **77**, 1–18.
113 J. Xu, X. Jie, F. Xie, H. Yang, W. Wei and Z. Xia, *Nano Res.*, 2018, **11**, 3648–3657.
114 X. Guo, D. Xu, H. Yuan, Q. Luo, S. Tang, L. Liu and Y. Wu, *J. Mater. Chem. A*, 2019, **7**, 27081–27088.
115 R. Liu, L. Dai, C. Si and Z. Zeng, *Carbohydr. Polym.*, 2018, **195**, 63–70.
116 Q. Yao, B. Fan, Y. Xiong, C. Jin, Q. Sun and C. Sheng, *Sci. Rep.*, 2017, **7**, 45914.
117 Q. Luo, X. Huang, Y. Luo, H. Yuan, T. Ren, X. Li, D. Xu, X. Guo and Y. Wu, *Chem. Eng. J.*, 2021, **407**, 127050.
118 F. Cheng, S. Zhang, L. Zhang, J. Sun and Y. Wu, *Colloids Surf., A*, 2022, **636**, 128149.
119 X.-C. Yang, Y.-L. Yang, M.-M. Xu, S.-S. Liang, X.-L. Pu, J.-F. Hu, Q.-L. Li, J.-T. Zhao and Z.-J. Zhang, *ACS Appl. Nano Mater.*, 2021, **4**, 13986–13994.
120 J. Yang, Y. Li, Y. Zheng, Y. Xu, Z. Zheng, X. Chen and W. Liu, *Small*, 2019, **15**, 1902826.
121 H. Maleki, *Chem. Eng. J.*, 2016, **300**, 98–118.
122 H. Maleki and N. Husing, *Appl. Catal., B*, 2018, **221**, 530–555.
123 S. Zhao, W. J. Malfait, N. Guerrero-Alburquerque, M. M. Koebel and G. Nystroem, *Angew. Chem., Int. Ed.*, 2018, **57**, 7580–7608.
124 L. Zhi, W. Zuo, F. Chen and B. Wang, *ACS Sustainable Chem. Eng.*, 2016, **4**, 3398–3408.
125 H. Yuan, G. Yang, Q. Luo, T. Xiao, Y. Zuo, X. Guo, D. Xu and Y. Wu, *Environ. Sci.: Nano*, 2020, **7**, 773–781.
126 Z. Song, X. Chen, X. Gong, X. Gao, Q. Dai, T. T. Nguyen and M. Guo, *Opt. Mater.*, 2020, **100**, 109642.
127 L. Jing, S. Yang, X. Li, Y. Jiang, J. Lou, Z. Liu, Q. Ding and W. Han, *Ind. Crop. Prod.*, 2022, **182**, 114882.
128 R. Li, W. Liang, M. Li, S. Jiang, H. Huang, Z. Zhang, J. J. Wang and M. K. Awasthi, *Int. J. Biol. Macromol.*, 2017, **104**, 1072–1081.
129 X. Li, M. Li, Q. Shi, H. Guo, L. Wang, X. Guo, Z. Chen, J. L. Sessler, H. Xiao and T. D. James, *Small*, 2022, **18**, 2201949.
130 J. Zhu, Q. Lu, C. Chen, J. Hu and J. Liu, *J. Mater. Chem. C*, 2017, **5**, 6917–6922.
131 L. Hu, B. Zhu, L. Zhang, H. Yuan, Q. Zhao and Z. Yan, *Analyst*, 2019, **144**, 474–480.
132 B. Kaur, N. Kaur and S. Kumar, *Coord. Chem. Rev.*, 2018, **358**, 13–69.
133 Y.-W. Lin, C.-C. Huang and H.-T. Chang, *Analyst*, 2011, **136**, 863–871.
134 S. Qin, X. Yu and L. Xu, *J. Hazard. Mater.*, 2021, **405**, 123978.
135 Z. Rahmani and M. Ghaemy, *Opt. Mater.*, 2019, **97**, 109356.
136 D. Xie, Y. Ma, Y. Gu, H. Zhou, H. Zhang, G. Wang, Y. Zhang and H. Zhao, *J. Mater. Chem. A*, 2017, **5**, 23794–23804.
137 M. Montalti, L. Prodi and N. Zaccheroni, *J. Mater. Chem.*, 2005, **15**, 2810–2814.
138 R. Tian, Y. Qu and X. Zheng, *Anal. Chem.*, 2014, **86**, 9114–9121.
139 X. Huang, Y. Wang, X. Liao and B. Shi, *J. Hazard. Mater.*, 2010, **183**, 793–798.
140 S. Qin, L.-y Ma, X. Sun, X. Mao and L. Xu, *J. Hazard. Mater.*, 2019, **366**, 529–537.
141 R. Xie, Y. Qu, M. Tang, J. Zhao, S. Chua, T. Li, F. Zhang, A. E. H. Wheatley and F. Chai, *Food Chem.*, 2021, **364**, 130366.
142 H.-B. Cheng, Z. Li, Y.-D. Huang, L. Liu and H.-C. Wu, *ACS Appl. Mater. Interfaces*, 2017, **9**, 11889–11894.
143 D. Dai, Z. Li, J. Yang, C. Wang, J.-R. Wu, Y. Wang, D. Zhang and Y.-W. Yang, *J. Am. Chem. Soc.*, 2019, **141**, 4756–4763.
144 I. Hisaki, C. Xin, K. Takahashi and T. Nakamura, *Angew. Chem., Int. Ed.*, 2019, **58**, 11160–11170.
145 M. A. Little and A. I. Cooper, *Adv. Funct. Mater.*, 2020, **30**, 1909842.
146 G. Singh, J. Lee, A. Karakoti, R. Bahadur, J. Yi, D. Zhao, K. AlBahily and A. Vinu, *Chem. Soc. Rev.*, 2020, **49**, 4360–4404.
147 A. G. Slater and A. I. Cooper, *Science*, 2015, **348**, aaa8075.
148 Q. Guan, L.-L. Zhou and Y.-B. Dong, *Chem. Soc. Rev.*, 2022, **51**, 6307–6416.

149 D. Rodriguez-San-Miguel, C. Montoro and F. Zamora, *Chem. Soc. Rev.*, 2020, **49**, 2291–2302.
150 S. Yuan, X. Li, J. Zhu, G. Zhang, P. Van Puyvelde and B. Van der Bruggen, *Chem. Soc. Rev.*, 2019, **48**, 2665–2681.
151 Y. Zhang, H. Li, J. Chang, X. Guan, L. Tang, Q. Fang, V. Valtchev, Y. Yan and S. Qiu, *Small*, 2021, **17**, 2006112.
152 H.-L. Qian, F.-L. Meng, C.-X. Yang and X.-P. Yan, *Angew. Chem., Int. Ed.*, 2020, **59**, 17607–17613.
153 G. Li, J. Ye, Q. Fang and F. Liu, *Chem. Eng. J.*, 2019, **370**, 822–830.
154 S.-Y. Ding, M. Dong, Y.-W. Wang, Y.-T. Chen, H.-Z. Wang, C.-Y. Su and W. Wang, *J. Am. Chem. Soc.*, 2016, **138**, 3031–3037.
155 Y. X. Yu, G. L. Li, J. H. Liu and D. Q. Yuan, *Chem. Eng. J.*, 2020, **401**, 126139.
156 W.-R. Cui, W. Jiang, C.-R. Zhang, R.-P. Liang, J. Liu and J.-D. Qiu, *ACS Sustainable Chem. Eng.*, 2020, **8**, 445–451.
157 Y. Lu, Y. Liang, Y. Zhao, M. Xia, X. Liu, T. Shen, L. Feng, N. Yuan and Q. Chen, *ACS Appl. Mater. Interfaces*, 2021, **13**, 1644–1650.
158 X. H. Xiong, Z. W. Yu, L. L. Gong, Y. Tao, Z. Gao, L. Wang, W. H. Yin, L. X. Yang and F. Luo, *Adv. Sci.*, 2019, **6**, 1900547.
159 W.-R. Cui, C.-R. Zhang, W. Jiang, F.-F. Li, R.-P. Liang, J. Liu and J.-D. Qiu, *Nat. Commun.*, 2020, **11**, 436.
160 X. Li, Y. Liu, J. Wang, J. Gascon, J. Li and B. Van der Bruggen, *Chem. Soc. Rev.*, 2017, **46**, 7124–7144.
161 M. Mon, R. Bruno, E. Tiburcio, M. Viciano-Chumillas, L. H. G. Kalinke, J. Ferrando-Soria, D. Armentano and E. Pardo, *J. Am. Chem. Soc.*, 2019, **141**, 13601–13609.
162 S. Wu, H. Min, W. Shi and P. Cheng, *Adv. Mater.*, 2020, **32**, 1805871.
163 M. Woellner, S. Hausdorf, N. Klein, P. Mueller, M. W. Smith and S. Kaskel, *Adv. Mater.*, 2018, **30**, 1704679.
164 X. Jia, M. Peydayesh, Q. Huang and R. Mezzenga, *Small*, 2022, **18**, 2105502.
165 Y. Peng, H. Huang, Y. Zhang, C. Kang, S. Chen, L. Song, D. Liu and C. Zhong, *Nat. Commun.*, 2018, **9**, 187.
166 N. D. Rudd, H. Wang, E. M. A. Fuentes-Fernandez, S. J. Teat, F. Chen, G. Hall, Y. J. Chabal and J. Li, *ACS Appl. Mater. Interfaces*, 2016, **8**, 30294–30303.
167 S.-W. Lv, J.-M. Liu, C.-Y. Li, N. Zhao, Z.-H. Wang and S. Wang, *Chem. Eng. J.*, 2019, **375**, 122111.
168 H. Yang, C. Peng, J. Han, Y. Song and L. Wang, *Sens. Actuators, B*, 2020, **320**, 128447.
169 L. Zhang, J. Wang, X. Ren, W. Zhang, T. Zhang, X. Liu, T. Du, T. Li and J. Wang, *J. Mater. Chem. A*, 2018, **6**, 21029–21038.
170 A. Radwan, I. M. El-Sewify, A. Shahat, H. M. E. Azzazy, M. M. H. Khalil and M. F. El-Shahat, *ACS Sustainable Chem. Eng.*, 2020, **8**, 15097–15107.
171 S. Safaei, H. Kazemian and P. C. Junk, *J. Solid State Chem.*, 2021, **300**, 122267.
172 S. Qin, X. He, F. Jin, Y. Wang, H. Chu, S. Han, Y. Sun and L. Gao, *RSC Adv.*, 2022, **12**, 18784–18793.
173 H. Guo, X. Wang, N. Wu, M. Xu, M. Wang, L. Zhang and W. Yang, *Anal. Methods*, 2020, **12**, 4058–4063.
174 L. Guo, Y. Song, K. Cai and L. Wang, *Spectrochim. Acta, Part A*, 2020, **227**, 117703.
175 Y. Ma, G. Xu, F. Wei, Y. Cen, Y. Ma, Y. Song, X. Xu, M. Shi, S. Muhammad and Q. Hu, *J. Mater. Chem. C*, 2017, **5**, 8566–8571.
176 L. Xu, G. Fang, J. Liu, M. Pan, R. Wang and S. Wang, *J. Mater. Chem. A*, 2016, **4**, 15880–15887.
177 M. R. Awual, *Chem. Eng. J.*, 2015, **266**, 368–375.
178 K. T. Kubra, M. S. Salman, M. N. Hasan, A. Islam, M. M. Hasan and M. R. Awual, *J. Mol. Liq.*, 2021, **336**, 116325.
179 M. R. Awual, *J. Environ. Chem. Eng.*, 2019, **7**, 103378.
180 M. R. Awual, *Mater. Sci. Eng., C*, 2019, **101**, 686–695.
181 M. R. Awual, M. M. Hasan, A. Shahat, M. Naushad, H. Shiwaku and T. Yaita, *Chem. Eng. J.*, 2015, **265**, 210–218.
182 K. T. Kubra, M. M. Hasan, M. N. Hasan, M. S. Salman, M. A. Khaleque, M. C. Sheikh, A. I. Rehan, A. I. Rasee, R. M. Waliullah, M. E. Awual, M. S. Hossain, A. K. D. Alsukaibi, H. M. Alshammari and M. R. Awual, *Colloids Surf., A*, 2023, **667**, 131415.
183 M. N. Hasan, M. S. Salman, M. M. Hasan, K. T. Kubra, M. C. Sheikh, A. I. Rehan, A. I. Rasee, M. E. Awual, R. M. Waliullah, M. S. Hossain, A. Islam, S. Khandaker, A. K. D. Alsukaibi, H. M. Alshammari and M. R. Awual, *J. Mol. Struct.*, 2023, **1276**, 134795.
184 M. R. Awual, *J. Environ. Chem. Eng.*, 2019, **7**, 103087.
185 M. R. Awual, *Chem. Eng. J.*, 2017, **307**, 85–94.
186 M. M. Hasan, K. T. Kubra, M. N. Hasan, M. E. Awual, M. S. Salman, M. C. Sheikh, A. I. Rehan, A. I. Rasee, R. M. Waliullah, M. S. Islam, S. Khandaker, A. Islam, M. S. Hossain, A. K. D. Alsukaibi, H. M. Alshammari and M. R. Awual, *J. Mol. Liq.*, 2023, **371**, 121125.
187 K. T. Kubra, M. S. Salman, M. N. Hasan, A. Islam, S. H. Teo, M. M. Hasan, M. C. Sheikh and M. R. Awual, *J. Mol. Liq.*, 2021, **338**, 116667.
188 M. S. Salman, M. N. Hasan, M. M. Hasan, K. T. Kubra, M. C. Sheikh, A. I. Rehan, R. M. Waliullah, A. I. Rasee, M. E. Awual, M. S. Hossain, A. K. D. Alsukaibi, H. M. Alshammari and M. R. Awual, *J. Mol. Struct.*, 2023, **1282**, 135259.
189 M. Xiao, Z. Liu, N. Xu, L. Jiang, M. Yang and C. Yi, *ACS Sens.*, 2020, **5**, 870–878.

